

AD 736633

Naval Warfare Research Center

Final Report - Phase IV

PENETRATION STUDIES OF ICE WITH APPLICATION TO ARCTIC AND SUBARCTIC WARFARE

By BERNARD ROSS SATHYA HANAGUD GURSHARAN SIDHU

Prepared for:

SUBMARINE ARCTIC WARFARE AND SCIENTIFIC PROGRAM
NAVAL ORDNANCE LABORATORY
SILVER SPRING, MARYLAND
AND
THE OFFICE OF NAVAL RESEARCH
WASHINGTON, D.C.

CONTRACT N00014-68-A-0243

DISTRIBUTION STATEMENT A
Approved for public release;
Distribution Unlimited

NWRC 7000-452-5

Reproduced by
NATIONAL TECHNICAL
INFORMATION SERVICE
Springfield Va 22151



STANFORD RESEARCH INSTITUTE
Menlo Park, California 94025 • U.S.A.

UNCLASSIFIED
Security Classification

DOCUMENT CONTROL DATA - R & D

(Security classification of title, body of abstract and indexing annotation must be entered when the overall report is classified)

1. ORIGINATING ACTIVITY (Corporate author) Stanford Research Institute 333 Ravenswood Avenue Menlo Park, California 94025		2a. REPORT SECURITY CLASSIFICATION UNCLASSIFIED	
		2b. GROUP	
3. REPORT TITLE PENETRATION STUDIES OF ICE WITH APPLICATION TO ARCTIC AND SUBARCTIC WARFARE			
4. DESCRIPTIVE NOTES (Type of report and inclusive dates) Final Report			
5. AUTHOR(S) (First name, middle initial, last name) Bernard Ross Sathya Hanagud Gursharan Sidhu			
6. REPORT DATE April 1971		7a. TOTAL NO. OF PAGES 82 69	7b. NO. OF REFS 18
8a. CONTRACT OR GRANT NO. N00014-68-A-0243		9a. ORIGINATOR'S REPORT NUMBER(S)	
b. PROJECT NO.			
c. NR 274-008-13		9b. OTHER REPORT NO(S) (Any other numbers that may be assigned this report)	
d.			
10. DISTRIBUTION STATEMENT			
11. SUPPLEMENTARY NOTES		12. SPONSORING MILITARY ACTIVITY Submarine Arctic Warfare and Scientific Program, NOL, Silver Spring, Md., and The Office of Naval Research, Washington, D.C.	
13. ABSTRACT Theoretical studies concerning the mechanics of penetration and perforation of a snow covered Arctic sea ice sheet subjected to projectile impact were performed. Penetration problems were treated by a deep penetration theory based on dynamic spherical cavity expansion analysis. In particular, finite compactibility and permanent deformation of both the snow and sea ice target materials were taken into account by assuming a locking approximation for behavior under hydrostatic stress, and response as an elastic-plastic, linear strain hardening solid under shear stress. Perforation problems were treated with the aid of a two-dimensional, large deformation, dynamic, elastic-plastic computer code (CANDIA CODE) which was developed in a previous investigation. Specifically, axi-symmetric, dynamic stress distributions were studied under conditions of impact at normal incidence for a cylindrical blunt end projectile and a sea ice target slab. A capability for considering perforation problems where fracture in the sea ice target material occurs was developed. In this connection, the redistributions of both tensile and shear stresses that accompany propagating fracture surfaces were acknowledged. The program was also modified to provide projectile deceleration loads during the perforation process, and subroutines were created to treat multilayer ice slabs and thereby accommodate effects contributed by overlying snow cover and the underlying mushy sea ice skeleton layer.			

DD FORM 1473 (PAGE 1)
1 NOV 68
S/N 0101-807-8801

UNCLASSIFIED
Security Classification

UNCLASSIFIED

Security Classification

14 KEY WORDS	LINK A		LINK B		LINK C	
	ROLE	WT	ROLE	WT	ROLE	WT
Arctic						
Antisubmarine Warfare						
Sea Ice						
Snow						
Frozen Ground						
Penetration						
Perforation						
Shaped Charges						
Dynamic Cavity Expansion Theory						
2-Dimensional Large Deformation, Elastic-Plastic						
Computer Code						
CANDIA CODE						
Elastic-Plastic Impact of Plates and Rods						
Compactible Materials						



STANFORD RESEARCH INSTITUTE
Menlo Park, California

*Naval Warfare Research Center
Final Report -- Phase IV*

April 1971

PENETRATION STUDIES OF ICE WITH APPLICATION TO ARCTIC AND SUBARCTIC WARFARE

By: BERNARD ROSS SATHYA HANAGUD GURSHARAN SIDHU

Prepared for:

SUBMARINE ARCTIC WARFARE AND SCIENTIFIC PROGRAM
NAVAL ORDNANCE LABORATORY
SILVER SPRING, MARYLAND
AND
THE OFFICE OF NAVAL RESEARCH
WASHINGTON, D.C.

CONTRACT N00014-68-A-0243
NR 274-008-13

SRI Project 7000-452

The work this report describes was performed by the Naval Warfare Research Center, Stanford Research Institute. It does not necessarily represent the conclusions or opinions of the Department of the Navy or any part thereof.

Reproduction of this document in whole or in part is permitted for any purpose of the United States Government.

Approved by:

LAWRENCE J. LOW, *Director*
Naval Warfare Research Center

ERNEST J. MOORE, *Executive Director*
Engineering Systems Division

NWRC 7000-452-5

ABSTRACT

Theoretical studies concerning the mechanics of penetration and perforation of a snow covered Arctic sea ice sheet subjected to projectile impact were performed.

Penetration problems were treated by a deep penetration theory based on dynamic spherical cavity expansion analysis. In particular, finite compactibility and permanent deformation of both the snow and sea ice target materials were taken into account by assuming a locking approximation for behavior under hydrostatic stress, and response as an elastic-plastic, linear strain hardening solid under shear stress.

Perforation problems were treated with the aid of a two-dimensional, large deformation, dynamic, elastic-plastic computer code (CANDIA CODE) which was developed in a previous investigation. Specifically, axisymmetric, dynamic stress distributions were studied under conditions of impact at normal incidence for a cylindrical blunt end projectile and a sea ice target slab. A capability for considering perforation problems where fracture in the sea ice target material occurs was developed. In this connection, the redistributions of both tensile and shear stresses that accompany propagating fracture surfaces were acknowledged. The program was also modified to provide projectile deceleration loads during the perforation process, and subroutines were created to treat multilayer ice slabs and thereby accommodate effects contributed by overlying snow cover and the underlying mushy sea ice skeleton layer.

PREFACE

The investigation reported here was sponsored by the U.S. Naval Ordnance Laboratory (NOL, White Oak), Silver Spring, Maryland, under ONR Contracts Nonr-2332(00) and N00014-68-A-0243 (SRI Project No. 7000-452). The work was performed between 1 July 1969 - 31 December 1969 and 15 April 1970 - 31 June 1970 and is designated, unofficially, Phase IV Study. Results of the ⁽¹⁹⁶⁹⁻¹⁹⁷⁰⁾ Phase I, ⁽¹⁹⁶⁹⁻¹⁹⁷⁰⁾ Phase II, and ⁽¹⁹⁶⁹⁻¹⁹⁷⁰⁾ Phase III studies were published in separate Stanford Research Institute reports under a similar title and dated November 1965, May 1967, and September 1969.

The contract was monitored for the Naval Ordnance Laboratory by Mr. M. M. Kleinerman. Project leader for Stanford Research Institute was Dr. Bernard Ross, and principal investigators were Dr. Sathya Hanagud, Dr. Bernard Ross, and Mr. Gursharan Sidhu.

CONTENTS

ABSTRACT	iii
PREFACE	v
LIST OF ILLUSTRATIONS	ix
LIST OF SYMBOLS	xi
 I INTRODUCTION	 1
II MECHANICS OF FRACTURE	5
III MECHANICS OF PENETRATION	11
 Appendix A LISTING FOR LARGE DEFORMATION THEORY COMPUTER CODE THAT INCORPORATES STRESS REDISTRIBUTIONS DUE TO FRACTURE	 37
REFERENCES	67

ILLUSTRATIONS

Fig. 1	Schematic Representation of Projectile Penetration Process in a Snow Covered Ice Sheet: Initial Entry and First Phase Motion	13
Fig. 2	Schematic Representation of Projectile Penetration Process in a Snow Covered Ice Sheet: Transition and Second Phase Motion	13
Fig. 3	Dynamic Cavity Expansion Problem for a Rigid Plastic, Ideal Locking Material	14
Fig. 4	Idealized Stress-Strain Curves for a Rigid Plastic, Ideal Locking Material with Linear Strain Hardening After Yield	14
Fig. 5	Dynamic Cavity Expansion Problem for an Elastic-Plastic, Incompressible Material	25
Fig. 6	Idealized Stress-Strain Curves for an Elastic-Plastic, Incompressible Material with Linear Strain Hardening After Yield	25

SYMBOLS

- A - cross-section area of projectile
- a - radius of spherical cavity, see Fig. 3
- B_1, B_2 - constants related to dynamic pressure, see Eq. III-34
- b - radius of spherical shock front, see Fig. 3
- C_0 - constant of integration
- C_1, C_2 - constants related to dynamic pressure, see Eq. III-77
- D - diameter of projectile
- E - modulus of elasticity (Young's modulus)
- E_t - tangent modulus for linear strain-hardening
- \bar{f} - limit of integration, see Eqs. III-8, III-41
- $f(t), g(t)$ - functions of integration
- k - radius of elastic-plastic spherical shock front, see Fig. 5
- M - mass of projectile
- n - summation exponent
- P_I - static pressure term given by Eq. III-52
- P_{II} - static pressure term given by Eq. III-72
- p_s - static pressure term given by Eq. III-34
- $p(t)$ - dynamic pressure applied to spherical cavity surface as a function of time

q, \dot{q}, \ddot{q} - depth, velocity, and acceleration, respectively, of projectile in target material

q_{os} - depth of projectile penetration at transition point, $q_{os} = R$

q_t - final penetration depth of projectile

R - depth of snow-ice interface at transition point of projectile penetration process, see Fig. 2

R_o - depth of snow cover, see Fig. 1

r - radial coordinate

r' - dummy variable of integration

t - time

V_o - velocity of projectile after completion of shallow penetration phase, assumed equal to impact velocity

v - outward particle velocity in radial direction

v_{os} - projectile velocity at transition point, equal to impact velocity for second phase of penetration

x - nondimensional quantity, $x = \xi^2$

Y - yield stress

y - nondimensional quantity, $y = 1/x$

α_p - ice parameter given by $\alpha_p = \left(1 - \frac{\rho_o}{\rho_{lp}}\right)$

$\bar{\alpha}_p$ - parameter given by $\bar{\alpha}_p = \left(1 - e^{-3\beta \frac{\rho_o}{\rho_{lp}}}\right)$

$$\alpha_s - \text{snow parameter given by } \alpha_s = \left(1 - \frac{\rho_{os}}{\rho_{ls}}\right)$$

$$\bar{\alpha}_s - \text{parameter given by } \bar{\alpha}_s = \left(1 - e^{-3\beta_s \frac{\rho_{os}}{\rho_{lp}}}\right)$$

$$\alpha_{ls} - \text{parameter given by } \alpha_{ls} = \left(1 - \frac{\rho_{lp}}{\rho_{ls}}\right)$$

$$\beta - \text{material parameter for ice given by } \beta = \frac{Y}{2E} - \frac{\bar{\epsilon}_l p}{3}$$

$$\beta_s - \text{material parameter for snow given by } \beta_s = \frac{Y_s}{2E_s} - \frac{\bar{\epsilon}_{ls}}{3}$$

ϵ - small quantity in the mathematical sense

$\epsilon_l, \bar{\epsilon}_l$ - locking strain, $\bar{\epsilon}_l = -\epsilon_l$

$\epsilon_r, \epsilon_\theta$ - normal strains in radial and circumferential directions, respectively

$\dot{\epsilon}_r, \dot{\epsilon}_\theta$ - normal strain rates in radial and circumferential directions, respectively

$$\eta - \text{series expression given by } \eta = \sum_{n=1}^{\infty} \frac{1}{n^2} \left(1 - e^{-3\beta \frac{\rho_o}{\rho_{lp}}}\right)^n$$

θ - equatorial spherical coordinate

ξ - nondimensional quantity, $\xi = r/a$

- ρ - density of target material
- ρ_l - locking density of target material
- σ_r, σ_θ - normal stresses in radial and circumferential directions, respectively

Subscripts

- p - refers to locked plastic region in sea ice
- o - refers to initial values and/or stress-free region
- s - refers to snow region
- I - refers to ice region
- 1, 2 - initial and final states, respectively, of a hydrostatic compression process

I INTRODUCTION

This report presents the final results of a comprehensive, long term investigation concerning the penetration and perforation* behavior of Arctic sea ice subjected to impact by inert projectiles. The importance of these engineering problems to the Arctic Antisubmarine Warfare Program has been described in three reports under the present title issued during November 1965,^{1**} May 1967,² and September 1969.³ The last report contained a complete summary of work performed and progress achieved up to that date; therefore, the topic is not considered anew.

However, it is noted briefly that two important analytical procedures for treating projectile-sea ice interaction problems were developed after completion of the second study. As described in the last report, these efforts included the realization of a large deformation, elastic-plastic, artificial viscosity type computer program (CANDIA CODE) which could be used to solve a wide variety of axisymmetric, two-dimensional, dynamic, and/or impact problems,^{4,5,6,7,8} and a large deformation deep penetration theory for analyzing projectile motion in compactible media.^{9,10,11,12}

Even though it was possible to derive a substantial body of information by applying these procedures to Arctic sea ice perforation

* For the purpose of this study, penetration can be defined as the entrance of a projectile into a target or ice cover without completing its passage through the body, whereas perforation implies the complete piercing of the target slab or ice cover by the projectile.

** Superscript numbers refer to references which are collected at the end of this report.

and penetration problems, it was recognized that further improvements were still required for practical application of the theoretical work.

For example, perforation of an Arctic sea ice cover by an impacting projectile creates fracture surfaces in the target material, and it is the resultant geometry of this process that describes both the mode of perforation and the associated value of critical impact velocity.* Moreover, important redistributions of stresses occur when fracture surfaces develop, and these changes affect both the failure phenomenon itself and the magnitudes of stress experienced by the impacting projectile. In this connection, the previous version of the code was capable of providing complete descriptions of both stress and deformation fields in the impacting bodies. It remained to postulate suitable failure criteria and expected crack propagation paths to define the global fracture pattern and the mechanism of projectile transit through the sea ice cover.

In consequence of the present work, it is possible now to track the actual failure configuration as a function of time after initial impact, and to acknowledge that the complement of both shear and cleavage fracture surface propagation paths is being influenced continuously by the developing fracture process.

On the other hand, the previous deep penetration theory was limited in application to homogeneous, isotropic media and thus was not suitable for cases involving a snow covered Arctic ice sheet. To correct this shortcoming, present research efforts were directed toward realization of a multilayer deep penetration theory to treat the practical projectile

* Critical velocity is defined as the minimum or threshold impact velocity for complete penetration, i.e., perforation.

penetration problem characterized by a two-layer, snow-ice target material. This work can be employed to obtain penetration performance curves for projectiles deployed in a typical Arctic environment.

In sum, these connected analyses (namely, direct treatment of the dynamic fracture problem and synthesis of a multilayer, large deformation, deep penetration theory) constitute the basis of this investigation. However, in addition to these studies a subsidiary effort concerning the determination of maximum deceleration loads experienced by a projectile during the sea ice perforation process was carried out. Unfortunately, numerical calculations for both of these problems could not be carried out due to a lack of funds for computer runs. Therefore, the significance of present developments as applied to the design and development of naval weapons for Arctic application could not be examined.

II MECHANICS OF FRACTURE

The work accomplished was concentrated on modifying and restructuring the CANDIA CODE to enable theoretical analysis of problems where fracture of the ice slab occurs. This phenomenon engenders redistributions of stresses in the target material, and accompanying effects in the magnitude and distributions of loads sustained by the impacting projectile. Thus, from an overall viewpoint, these efforts were directed toward the transformation of a computer code employed previously as a research tool to a working code which can be utilized to perform engineering design and development calculations.

To sustain these particular goals and to treat the fracture problem in sea ice, per se, it was necessary to recast the code so that problems characterized by greater numbers of variables and finer finite-difference calculation mesh networks could be accommodated. For example, in initial format the code considered sea ice to be homogeneous and isotropic, whereas, in fact, this material is strongly anisotropic and inhomogeneous. Consequently, introduction of this more advanced description of material composition would furnish a demand for increase in the number of input variables that are needed for numerical calculation. Moreover, greater machine storage and capability were also required because a developing fracture surface submits many more mesh points of importance into the calculation process. To overcome these difficulties, the entire CANDIA CODE, as listed and flow-charted in the last comprehensive report,³ was restructured to eliminate its dependence on high speed core memory storage. As a result, the code in its present format can be employed to take advantage of random access disc storage.

Preceding page blank

At this time, the entire code exists on disc in precompiled form which is compatible with all electronic data processing equipment based on the FORTRAN language. As such, the code gains advantage in capability and versatility by employing fixed or consistent amounts of high speed core storage with a random access interface.

Briefly, advantages of the new disc format are:

- Capacity increased; that is, problems characterized by greater numbers of intrinsic variables and requiring finer mesh works for calculation purposes can be treated. The fracture problem in sea ice falls within this definition.
- Convenience increased; that is, ease of working with the code has been considered. For instance, the code is transcribed presently on one disc pack in lieu of multiple racks of perforated cards.
- Versatility increased; that is, interrupted calculations can be performed so that when a computation procedure is stopped intermittently it is no longer necessary to resume calculations from the initial, or zero, input state. Instead, numerical treatment can be restarted from the previous termination point. In this manner, and with particular relevance to the fracture problem, an analysis can be intercepted to focus attention on the development of a propagating fracture surface and the attendant stresses in plastic zones surrounding a crack tip.
- Information display possibilities increased; that is, direct computer readout is feasible to furnish continuing computer code output by means of cathode ray terminals. Thus, it becomes practical to take movies of progressive display patterns and thereby indicate visually the continuing propagation of fracture surfaces and ancillary stress redistributions in both target material and impacting projectile.

With restructuring and modification of the computer code effected, it was possible to attack the fracture problem directly. However, in

this case it was acknowledged first that the treatment of stress redistributions due to developing fracture surfaces would be closely coupled to the states of stress existing on free surface boundaries such that the proper numerical treatment of boundary conditions themselves would be an utmost necessity. In this connection, it was pointed out in Ref. 3 that many large deformation elastic-plastic computer codes currently in existence were founded on incorrect boundary condition formulations. Thus, an appendix was included in the report containing a lengthy derivation for the true treatment of these boundary conditions. Because this development was somewhat unwieldy in the form presented, considerable effort was expended during the current period in rewriting a more concise and simplified algorithm for this aspect of the problem.

Once this task was completed, it was possible to create an additional algorithm to treat the fracture problem itself. In this case, the algorithm was founded on the development of a point condition code which enabled integer point condition values to be associated with different characteristic free surface points on nodal intersections in the finite difference network. For example, individual point values were ascribed with concomitant subroutines to represent lateral and transverse free surface points, interior fracture surface points, and corner points on both target and projectile. As a result, point condition changes could be related to responsive subroutines in correspondence with physical transformations of both impacting bodies. Consequently, it is possible now to track in the computer both current boundary states and conditions, as well as emerging and propagating fracture surfaces.

Use was then made of the modified boundary condition and fracture algorithms to treat the shear fracture problem encountered when a blunt or hemispherical nose projectile experiences initial penetration in a target material. In this case, it was known from previous experimental,

field test, and theoretical studies that, due to the anisotropic nature of a sea ice target material, initial fracture under these impact conditions would occur in the shear mode along σ_{zz} -normal stress planes in the vertical direction.*

With the shear fracture phase of the overall perforation process accounted for, work progressed toward realization of a fracture algorithm to describe failure surface propagation under tensile principal stresses. The important difficulty overcome in treating this problem was that fracture does not occur necessarily along a mesh direction.** Therefore, there remained the burden of outlining and defining not only the stress redistributions at incipient fracture but the directions of the fracture planes themselves.

In this context, a method of approach was devised and implemented in the present version of the code. Specifically, all components of the σ_{ij}

* Fracture configurations in the shear mode are initiated upon projectile impact at normal incidence because, for a blunt penetrator, regions of intense shear stress are generated around the projectile periphery. Moreover, laboratory experiments and field test results, as well as theoretical calculations (CANDIA CODE), indicate that continued shear penetration and concomitant fracture patterns are engendered in the sea ice slab until penetration depths of the order of 70-80% sea ice sheet thickness are achieved. At this point, it is recognized that shear stress magnitudes fall off and that further fracture and ultimate perforation are the result of sea ice failure under tensile stress. In sum, complete penetration is obtained through a composite process characterized by initial failure due to shear and terminal failure as a result of tensile or cleavage fracture. Consequently, ultimate perforation results in the ejection of a cylindrical-conical shear plug of target material by the impacting body.

** In this connection, the orientations of component segments of a developing tensile fracture surface are related directly to the magnitudes and directions of local principal stresses, which themselves are dependent variables of the problem in question. Thus, developing cleavage fracture surfaces do not correspond necessarily in spatial alignment and configuration to the postulated geometry of the mesh network employed for finite-difference calculations.

stress tensor are determined at the center point of a given area segment in a mesh network. Knowing these quantities enables the three principal stresses to be determined, whereupon a test is performed to isolate any possibility that the shear stress component of the total stress tensor violates the allowable shear failure stress of the target material. Assuming this is not the case and that shear fracture does not develop, then the calculation sequence is pursued further by comparing the maximum principal stress value with the allowable failure stress in uniaxial tension. If the former quantity exceeds the latter, it can be assumed (i.e., at least for an elastic brittle material such as freshwater ice) that fracture occurs over the mesh section of interest. Then, spatial orientation of the fracture surface segment is obtained by considering the cleavage plane to be orthogonal to the direction of the maximum principal stress component.

Thus, knowledge of the magnitudes and directions of principal stress quantities at a central point in the mesh section enables the prediction of fracture likelihood and resultant local failure surface geometry to be made. Once fracture occurs over a mesh section, it is necessary to postulate free surface boundary conditions which provide a zero traction state over the developing area of material separation. Then, the physical situation at the failed mesh section must be rechecked at each and every time step of succeeding numerical calculation to determine whether changes in external loading and/or internal stress state have resulted in subjecting the mutual fracture surfaces to closure and compressive pressure. If this turns out to be the case, free surface boundary conditions are stricken and appropriate interface conditions substituted in their place. Finally, at the conclusion of each calculation time step, a locus or contour is passed through all of the individual fracture surface segments to indicate instantaneous states of the composite failure pattern developed in the target material subjected to projectile impact.

III MECHANICS OF PENETRATION

In addition to continuing research in the fracture problem, efforts were devoted to realizing a theory for the deep penetration of projectiles in multilayered media such as a snow covered Arctic sea ice sheet.^{13,14,15} Solutions of the deep penetration problem for a single layer, homogeneous, isotropic sea ice cover have been obtained already, and their formulation and development were presented in a recently issued comprehensive report.³ Fortunately, most of this previous work was applicable directly to the multilayered penetration problem; thus, the compounding of a tractable theory applicable to projectile-sea ice interaction problems for a more complicated target material did not offer substantial difficulty.

In this case, continued use was made of the two most important conceptual fundamentals upon which the previous theory was based. These are: first, that transformation of the deep penetration problem itself can be effected successfully to yield a problem concerned with dynamic stress distributions in an infinite solid that contains a spherical cavity subjected to step input in pressure*, and, second, that the dynamic constitutive behavior of compactible materials such as Arctic sea ice and snow can be represented satisfactorily by assuming an idealized locking approximation for Rankine-Hugoniot material behavior under hydrostatic compressive stress.

* This metamorphosis is founded specifically on the assumption that dynamic pressure experienced by a penetrating projectile at its stagnation point is comparable by reason of symmetry to the similar pressure quantity which exists at the surface of a dynamic expanding spherical cavity. A corollary assumption enables an expression for the complete force resisting continued penetration to be established by postulating that the spatial variation of pressure over the frontal portion of the projectile can be represented by a simple cosine relationship.¹⁷

Both of these arguments were invoked to resolve the multilayer penetration problem. In particular, a systematic approach was devised to recast the two-layer target configuration into the form of an idealized infinite body that included a spherical cavity surrounded by two concentric spherical regions of material having the relevant physical and mechanical properties of Arctic snow and sea ice. Then, the dynamic spherical expansion problem was worked through again for the composite material configuration. This task demanded relatively more complicated algebraic formulations but did not require an increase in mathematical generality or important theoretical innovation. The problem was made somewhat easier by the fact that reflected stress waves in a locked material travel at infinite speeds, so that introduction of limiting conditions into the mathematical process resulted in well-defined simplifications.

The problem considered is depicted schematically in Figs. 1 and 2. Attention is directed first to the ideal locked-rigid plastic material in Region 1_s (Figs. 3 and 4) which is behind the advancing shock front at $r = b(t)$. The locking condition on strain is

$$\epsilon_r + 2\epsilon_\theta = \epsilon_{l_s} \quad (\text{III-1})$$

where ϵ_{l_s} the ideal locking strain for snow is a time-invariant material property. Differentiating with respect to time results in

$$\dot{\epsilon}_r + 2\dot{\epsilon}_\theta = 0 \quad (\text{III-2})$$

These strain rate quantities can be expressed in terms of radial outward particle velocity, $v(r,t)$, by the kinematic relations

$$\dot{\epsilon}_r = \frac{\partial v}{\partial r} \quad \dot{\epsilon}_\theta = \frac{v}{r} \quad (\text{III-3})$$

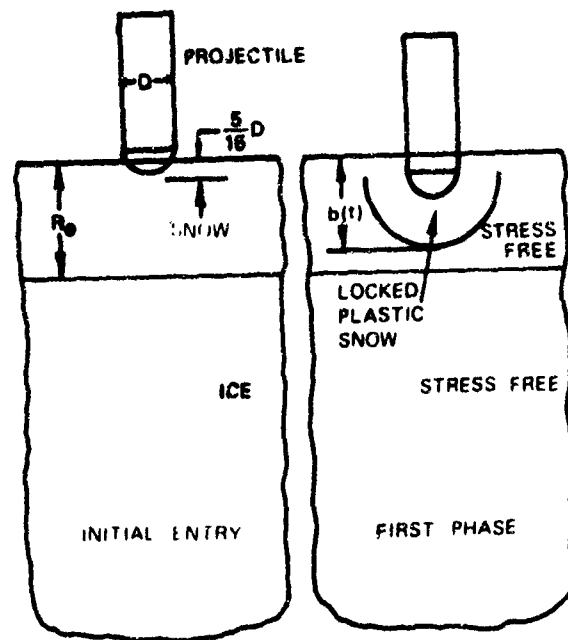


FIGURE 1 SCHEMATIC REPRESENTATION OF PROJECTILE PENETRATION PROCESS IN SNOW COVERED ICE SHEET. INITIAL ENTRY AND FIRST PHASE MOTION

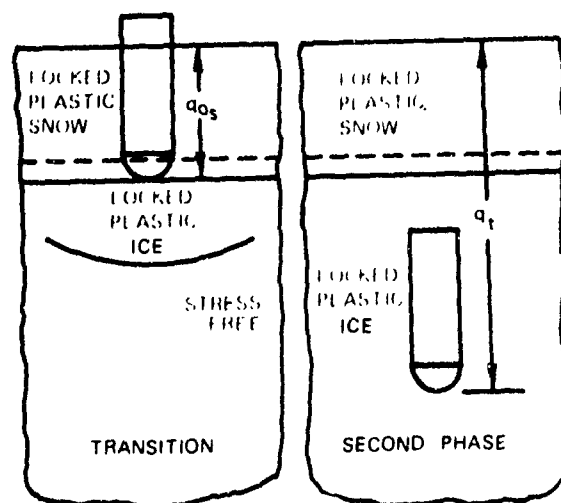


FIGURE 2 SCHEMATIC REPRESENTATION OF PROJECTILE PENETRATION PROCESS IN SNOW COVERED ICE SHEET. TRANSITION AND SECOND PHASE MOTION

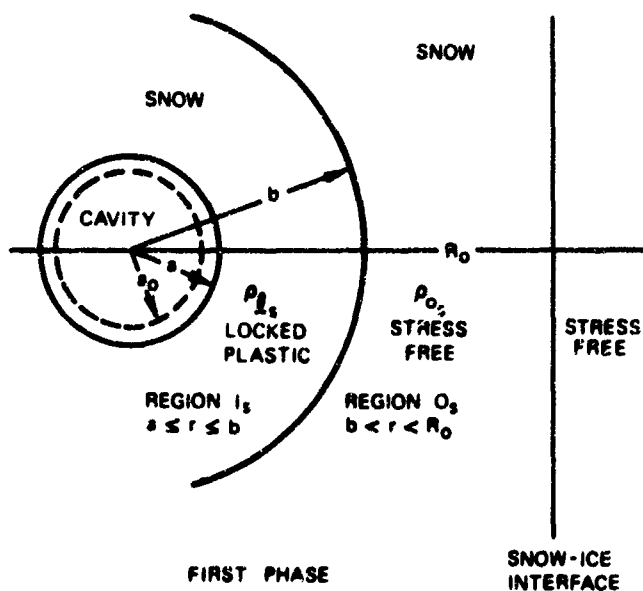


FIGURE 3 DYNAMIC CAVITY EXPANSION PROBLEM FOR A RIGID PLASTIC, IDEAL LOCKING MATERIAL

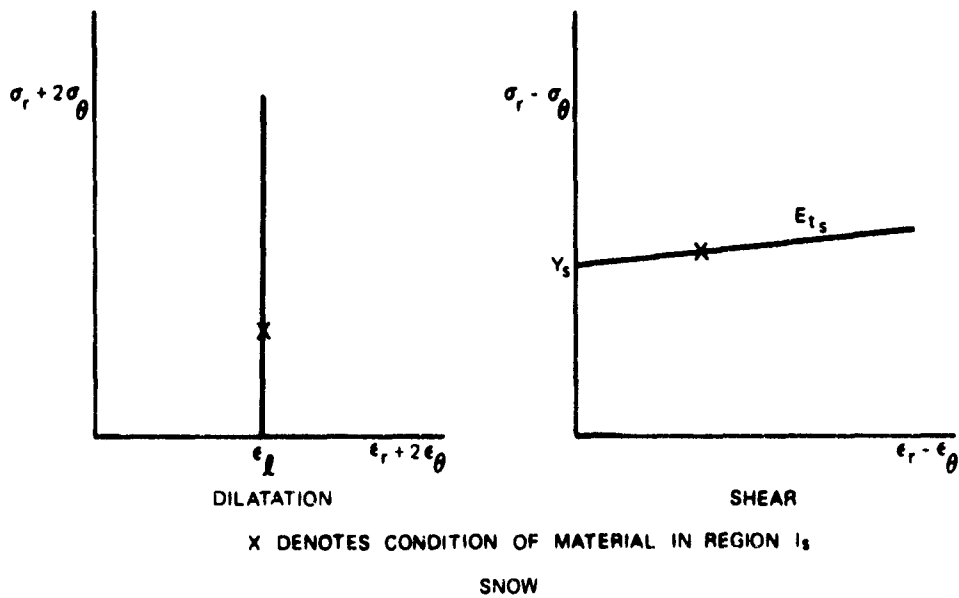


FIGURE 4 IDEALIZED STRESS-STRAIN CURVES FOR A RIGID PLASTIC, IDEAL LOCKING MATERIAL WITH LINEAR STRAIN HARDENING AFTER YIELD

Substitution and integration yield

$$v_s = \frac{f_s(t)}{r^2} \quad (\text{III-4})$$

where subscript s denotes quantities in the locked-plastic snow region. The stress-strain relationship in shear for a rigid-plastic material with linear strain hardening is³

$$\sigma_\theta - \sigma_r = Y_s + \frac{2}{3} E_{ts} (\epsilon_\theta - \epsilon_r) \quad (\text{III-5})$$

Under conditions of spherical symmetry, the equation of motion becomes

$$\frac{\partial \sigma_r}{\partial r} + \frac{2}{r} (\sigma_r - \sigma_\theta) = \rho_{ls} \left(\frac{\partial v_s}{\partial t} + v_s \frac{\partial v_s}{\partial r} \right) \quad (\text{III-6})$$

Finally, the large deformation circumferential strain is given by

$$\epsilon_\theta = \ln \frac{r}{r_o} \quad (\text{III-7})$$

Combining these relationships into Eq. III-6 and integrating provides the following expression.

$$\begin{aligned} \sigma_{rs} = & 2Y_s \ln r + 2 \int_{\bar{f}_s}^r \frac{1}{r'} E_{ts} \left(2 \ln \frac{r'}{r_o} + \frac{2\bar{\epsilon}_{ls}}{3} \right) dr' \\ & - \rho_{ls} \frac{\dot{f}_s}{r} + \frac{1}{2} \rho_{ls} \frac{\dot{f}_s^2}{r^4} + g_s(t) \end{aligned} \quad (\text{III-8})$$

Conservation of mass across the shock front at the stress free-locked plastic interface yields

$$\rho_{os} \dot{b} = \rho_{ls} (\dot{b} - v_s) \quad @ \quad r = b(t) \quad (\text{III-9})$$

or upon reduction

$$f_s(t) = \alpha_s b^2 \dot{b} \quad (\text{III-10})$$

where

$$\alpha_s = 1 - \rho_{0s}/\rho_{ls} \quad (\text{III-11})$$

Similarly, conservation of momentum yields

$$\sigma_{rs} = -\rho_{ls}(\dot{b} - v_s)v_s \quad @ \quad r = b(t) \quad (\text{III-12})$$

or upon reduction

$$\sigma_{rs} \Big|_{r=b} = -\rho_{0s} \alpha_s \dot{b}^2 \quad (\text{III-13})$$

The boundary condition on stress at the cavity surface is

$$\sigma_{rs} = -p(t) \quad @ \quad r = a(t) \quad (\text{III-14})$$

Then, from Eq. III-8 evaluated at $r = a(t)$

$$\begin{aligned} g_s(t) = & -p(t) - 2Y_s \ln a - 2 \int_{\bar{r}_s}^a \frac{1}{r'} E_{ts} \left(2 \ln \frac{r'}{r_o} + \frac{2\bar{e}_{ls}}{3} \right) dr' \\ & + \rho_{ls} \frac{\dot{f}_s}{a} - \frac{1}{2} \rho_{ls} \frac{f_s^2}{a^4} \end{aligned} \quad (\text{III-15})$$

so that the equation for radial stress becomes

$$\begin{aligned}\sigma_{r_s} = & -p(t) + 2Y_s \ln \frac{r}{a} + 2 \int_a^r \frac{1}{r'} E_{ts} \left(2 \ln \frac{r'}{r_o} + \frac{2\bar{\epsilon}_s}{3} \right) dr' \\ & + \rho_{ls} \alpha_s \left(b^2 \ddot{b} + 2b\dot{b}^2 \right) \left(\frac{1}{a} - \frac{1}{r} \right) \\ & - \frac{1}{2} \rho_{ls} \alpha_s^2 b^4 \dot{b}^2 \left(\frac{1}{a^4} - \frac{1}{r^4} \right)\end{aligned}\quad (\text{III-16})$$

Using Eq. III-13, an expression is obtained for the pressure variation with time at the cavity surface

$$\begin{aligned}p(t) = & 2Y_s \ln \frac{b}{a} + 2 \int_a^b \frac{1}{r'} E_{ts} \left(2 \ln \frac{r'}{r_o} + \frac{2\bar{\epsilon}_s}{3} \right) dr' \\ & + \alpha_s \rho_{ls} \left(b^2 \ddot{b} + 2b\dot{b}^2 \right) \left(\frac{1}{a} - \frac{1}{b} \right) \\ & - \frac{1}{2} \alpha_s^2 \rho_{ls} b^4 \dot{b}^2 \left(\frac{1}{a^4} - \frac{1}{b^4} \right) + \rho_{os} \alpha_s \dot{b}^2\end{aligned}\quad (\text{III-17})$$

Equation III-17 can be reduced further by application of the boundary condition on particle velocity at the cavity surface

$$v_s = \dot{a} \quad @ \quad r = a(t) \quad (\text{III-18})$$

Using Eqs. III-4, III-10 results in

$$\alpha_s b^2 \dot{b} = a^2 \dot{a} \quad (\text{III-19})$$

Differentiation of both sides of Eq. III-19 with respect to time yields

$$\alpha_s (b^2 \ddot{b} + 2b\dot{b}^2) = a^2 \ddot{a} + 2a\dot{a}^2 \quad (\text{III-20})$$

Substitution of these results into Eq. III-17 gives

$$\begin{aligned} p(t) = & 2Y_s \ln \frac{b}{a} + 2 \int_a^b \frac{1}{r'} E_{ts} \left(2 \ln \frac{r'}{r_o} + \frac{2\bar{\epsilon}_{ls}}{3} \right) dr' \\ & + \rho_{ls} (a^2 \ddot{a} + 2a\dot{a}^2) \left(\frac{1}{a} - \frac{1}{b} \right) \\ & - \frac{1}{2} \rho_{ls} a^4 \dot{a}^2 \left(\frac{1}{a^4} - \frac{1}{b^4} \right) + \rho_{os} \frac{a^2}{b^2} \dot{a} \dot{b} \end{aligned} \quad (\text{III-21})$$

Surfaces of discontinuity in displacement and particle velocity cannot exist if fracture at the shock front is omitted from consideration. Thus, $v_s(t)$ is zero on the shock front since the stress free material ahead of the locked plastic zone is quiescent. As a consequence, no material moves through the shock front and the following compressibility relationship can be applied at successive times over the volume of locked plastic material bounded by the cavity surface and an arbitrary spherical surface at the present shock front location

$$(b^3 - a^3) \rho_{ls} = (b^3 - a_o^3) \rho_{os} \quad (\text{III-22})$$

Upon reduction

$$\alpha_s \frac{b^3}{a^3} = 1 - \frac{a_o^3}{a^3} \frac{\rho_{os}}{\rho_{ls}} \quad (\text{III-23})$$

But, it has been shown by Goodier^{16,17,18} that, for the deep penetration problem, the following assumption can be made

$$a^3 \gg a_0^3$$

In addition, $\rho_l > \rho_o$, so that

$$b^3 \approx \frac{1}{\alpha_s} a^3 \quad (\text{III-24})$$

Equation III-21 becomes

$$\begin{aligned} p(t) = & -\frac{2}{3} Y_s \ln \alpha_s + 2 \int_a^b \frac{1}{r'} E_{ts} \left(2 \ln \frac{r'}{r_o} + \frac{2\bar{\epsilon}_s}{3} \right) dr' \\ & + \rho_{ls} \left(a\ddot{a} + 2\dot{a}^2 \right) \left(1 - \alpha_s^{1/3} \right) \\ & - \frac{1}{2} \rho_{ls} \dot{a}^2 \left(1 - \alpha_s^{4/3} \right) + \rho_{os} \dot{a}^2 \alpha_s^{1/3} \end{aligned} \quad (\text{III-25})$$

The remaining integral must be evaluated. Application of an appropriate compressibility relationship at an arbitrary location, r , within the locked plastic region yields

$$(r^3 - a^3) \rho_{ls} = (r_o^3 - a_o^3) \rho_{os} \quad (\text{III-26})$$

Using the deep penetration assumption (i.e., $a^3 \gg a_0^3$), Eq. III-26 becomes*

$$\frac{r}{r_0} = \left[\frac{\rho_{os}}{\rho_{ls}} \frac{r^3/a^3}{r^3/a^3 - 1} \right]^{1/3} \quad (\text{III-27})$$

Letting

$$x = \xi^3 = r^3/a^3$$

and employing Eq. III-27 enables the integral expression in Eq. III-25 to be written as follows

$$\begin{aligned} & 2 \int_{a(t)}^{b(t)} \frac{1}{r'} E_{ts} \left(2 \ln \frac{r'}{r_0} + \frac{2\bar{\epsilon}_{ls}}{3} \right) dr' \\ &= \frac{4}{9} E_{ts} \left\{ \int_1^{b^3/a^3} \ln \frac{\rho_{os}}{\rho_{ls}} \frac{dx}{x} + \int_1^{b^3/a^3} \bar{\epsilon}_{ls} \frac{dx}{x} + \int_1^{b^3/a^3} \ln \frac{x}{x-1} \frac{dx}{x} \right\} \quad (\text{III-28}) \end{aligned}$$

*

$$(r^3 - a^3) \rho_{ls} = (r_0^3 - a_0^3) \rho_{os}$$

$$r^3 - a^3 = (r_0^3 - a_0^3) \rho_{os}/\rho_{ls}$$

$$r^3 - a^3 = r_0^3 \frac{\rho_{os}}{\rho_{ls}} - a_0^3 \frac{\rho_{os}}{\rho_{ls}}$$

$$\frac{r^3}{r_0^3} - \frac{a^3}{r_0^3} = \frac{\rho_{os}}{\rho_{ls}} - \frac{a_0^3}{r_0^3} \frac{\rho_{os}}{\rho_{ls}}$$

(footnote continued on next page)

Evaluation of the first two integrals in the second member of Eq. III-28 is straightforward.³ The remaining integral is attacked by letting $y = 1/x$ and changing the lower limit of integration to $1-\epsilon$ where $\epsilon \ll 1$. There results

$$\int_1^{b^3/a^3} \ln \frac{x}{x-1} \frac{dx}{x} \rightarrow \int_{1-\epsilon}^{a^3/b^3} \ln (1-y) \frac{dy}{y} \quad (\text{III-29})$$

Since $b > a$ always and $1-\epsilon < 1$, the range of values over which integration takes place (i.e., $1-\epsilon \geq y \geq b^3/a^3$) ensures that $y < 1$ so that the integrand can be expanded in series form. Step by step integration yields

$$\int_1^{b^3/a^3} \ln \frac{x}{x-1} \frac{dx}{x} = \left[y + \frac{y^2}{4} + \frac{y^3}{9} + \dots \right]_{a^3/b^3}^{1-\epsilon} \quad (\text{III-30})$$

* (footnote continued)

but $\rho_{ls} > \rho_{os}$ and $r_o^3 \gg a_o^3$

$$\therefore \frac{(\rho_{os}/\rho_{ls})}{r^3/r_o^3 - a^3/r_o^3} = 1$$

$$\frac{(\rho_{os}/\rho_{ls}) r^3}{r^3/r_o^3 - a^3/r_o^3} = r^3$$

$$\frac{(\rho_{os}/\rho_{ls}) r^3 r_o^3}{r^3 - a^3} = r^3$$

$$\therefore \frac{r^3}{r_o^3} = \frac{(\rho_{os}/\rho_{ls}) r^3/a^3}{r^3/a^3 - 1}$$

Allowing $\epsilon \rightarrow 0$ and introducing Eq. III-24 results in

$$\int_1^{b^3/a^3} \ln \frac{x}{x-1} \frac{dx}{x} = \frac{\pi^2}{6} - \sum_{n=1}^{\infty} \frac{1}{n^2} \alpha_s^n \quad (\text{III-31})$$

Finally, Eq. III-25 becomes

$$\begin{aligned} p(t) = & -\frac{2}{3} Y_s \ln \alpha_s + \frac{4}{9} E_{ts} \left(\frac{\pi^2}{6} - \sum_{n=1}^{\infty} \frac{1}{n^2} \alpha_s^n \right) \\ & + \rho_{ls} (a\ddot{a} + 2\dot{a}^2) (1 - \alpha_s^{1/3}) \\ & - \frac{1}{2} \rho_{ls} \dot{a}^2 (1 - \alpha_s^{4/3}) + \rho_{os} \dot{a}^2 \alpha_s^{1/3} \end{aligned} \quad (\text{III-32})$$

The expression for pressure can be broken down into static and dynamic parts so that

$$p(t) = p_s + \rho_{ls} (B_1 a\ddot{a} + B_2 \dot{a}^2) \quad (\text{III-33})$$

where

$$p_s = \frac{2}{27} \pi^2 E_{ts} - \frac{2}{3} Y_s \ln \alpha_s - \frac{4}{9} E_{ts} \sum_{n=1}^{\infty} \frac{1}{n^2} \alpha_s^n$$

$$B_1 = 1 - \alpha_s^{1/3}$$

$$B_2 = \frac{3}{2} - (1 + \alpha_s) \alpha_s^{1/3} + \frac{1}{2} \alpha_s^{4/3}$$

or

$$B_2 = \frac{3}{2} - \alpha_s^{1/3} - \frac{1}{2} \alpha_s^{4/3} \quad (\text{III-34})$$

The relationship for pressure variation at the cavity surface given by Eq. III-33 is used in the Goodier deep penetration theory^{3,16} to obtain an expression for resisting forces acting on the projectile. Then, an equation of motion for projectile transit in the target material can be written

$$M\ddot{q} = - \left\{ p_S + \frac{2}{3} \rho \ell_s \left(B_1 \frac{D}{2} \ddot{q} + B_2 \dot{q}^2 \right) \right\} \frac{\pi D^2}{4} \quad (\text{III-35})$$

After integration, Eq. III-35 becomes

$$\ln \left(p_S + \frac{2}{3} B_2 \rho \ell_s \dot{q}^2 \right) = - \frac{4}{3} B_2 \rho \ell_s \frac{q}{\frac{M}{A} + B_1 \frac{D}{3} \rho \ell_s} + C_0 \quad (\text{III-36})$$

Exact shallow penetration theory^{3,16} is avoided in this consideration. Instead, it is assumed on balance that the onset of resistance to penetration in snow takes place at an indentation depth corresponding to the centroid of the nose hemisphere. That is, when $q = 5D/16$. Under these conditions, Eq. III-36 becomes

$$\ln \frac{p_S + \frac{2}{3} B_2 \rho \ell_s \dot{q}^2}{p_S + \frac{2}{3} B_2 \rho \ell_s V_o^2} = - \frac{4}{3} \frac{B_2 \rho \ell_s}{\frac{M}{A} + B_1 \frac{D}{3} \rho \ell_s} (q - 5D/16) \quad (\text{III-37})$$

The first phase of penetration is completed when the projectile encounters the snow-ice interface. Here,

$$q = q_{0s} = R \gtrsim R_o$$

Substitution of $q = R$ into Eq. III-37 determines the projectile velocity, \dot{q}_{0s} , which characterizes initiation of the second penetration phase.

In the second phase of penetration, the projectile encounters an ice cover which is assumed in the present problem to behave as an elastic-plastic solid in shear, and incompressible under hydrostatic stress. Attention is directed to Figs. 5 and 6. Using expressions which have been developed in Ref. 3, the radial normal stress at the snow-ice interface is given by*

$$\begin{aligned}
 -\sigma_{rI}\bigg|_{r=R} = & -\frac{2}{3} Y \ln\left(1 - e^{-3\beta} \frac{\rho_o}{\rho_{lp}}\right) + \frac{2}{27} \pi^2 E_t \\
 & - \frac{4}{9} E_{ts} \sum_{n=1}^{\infty} \frac{1}{n^2} \left(1 - e^{-3\beta} \frac{\rho_o}{\rho_{lp}}\right)^n \\
 & + \frac{4}{9} E \left(1 - e^{-3\beta}\right) + \alpha_p \rho_o \dot{b}^2 \\
 & + \alpha_p \rho_{lp} (b\ddot{b} + 2\dot{b}^2) \left(\frac{b}{R} - 1\right) \\
 & - \frac{1}{2} \alpha_p^2 \rho_{lp} \dot{b}^2 \left(\frac{b^4}{R^4} - 1\right)
 \end{aligned} \tag{III-38}$$

Again, from previous work

$$v_I\bigg|_{r=R} = \alpha_p \frac{b^2 \dot{b}}{R^2} = \frac{f_I(t)}{R^2} \tag{III-39}$$

$$\text{where} \quad f_I(t) = \alpha_p b^2 \dot{b} \tag{III-40}$$

* The subscript, I, has been omitted from the quantities Y , ρ_o , ρ_{lp} , E_t , and E for reasons of mathematical convenience.

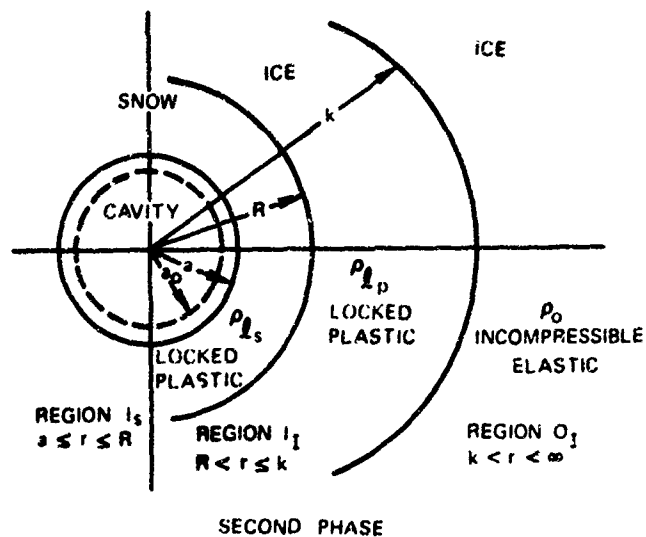


FIGURE 5 DYNAMIC CAVITY EXPANSION PROBLEM FOR AN ELASTIC-PLASTIC, INCOMPRESSIBLE MATERIAL

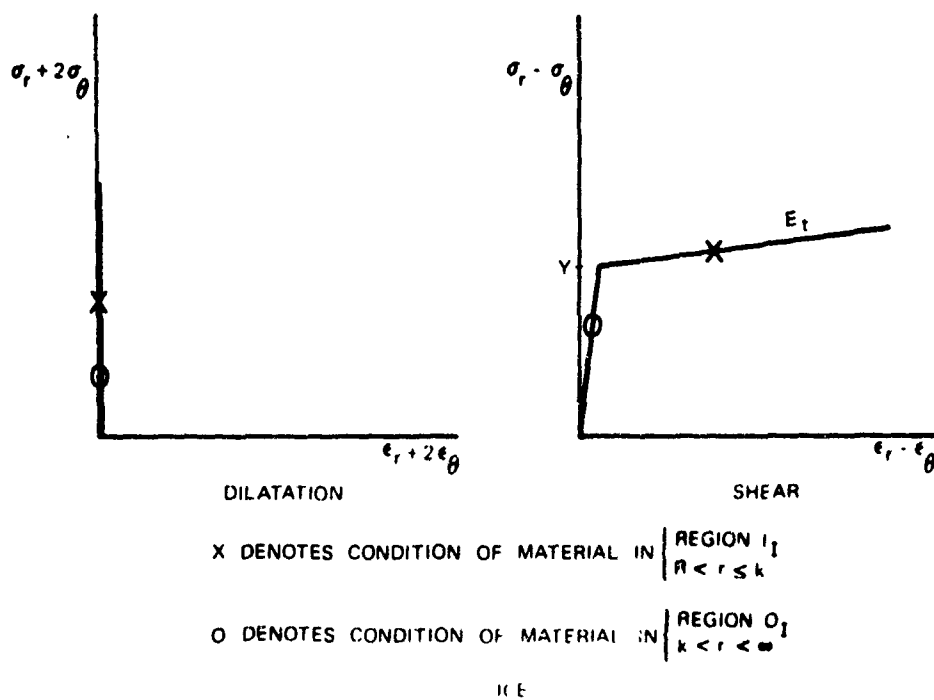


FIGURE 6 IDEALIZED STRESS-STRAIN CURVES FOR AN ELASTIC-PLASTIC, INCOMPRESSIBLE MATERIAL WITH LINEAR STRAIN HARDENING AFTER YIELD

In the snow region, the general solution to the problem can be written as

$$\begin{aligned} \sigma_{r_s} = & 2Y_s \ln r + 2 \int_{\bar{f}_s}^r \frac{1}{r'} E_{t_s} \left(2 \ln \frac{r'}{r_o} + \frac{2}{3} \bar{\epsilon}_{\ell_s} \right) dr' \\ & - \rho_{\ell_s} \frac{\dot{f}_s}{r} + \frac{1}{2} \rho_{\ell_s} \frac{r_s^2}{r^4} + g_s(t) \end{aligned} \quad (\text{III-41})$$

$$v_s = \frac{f_s(t)}{r^2} \quad (\text{III-42})$$

Boundary conditions are given by:

$$\begin{aligned} r &= a(t) \\ \sigma_{r_s} &= -p(t) \end{aligned} \quad (\text{III-43})$$

$$\begin{aligned} r &= R(t) \\ \rho_{\ell_s} (\dot{R} - v_s) &= \rho_{\ell_p} (\dot{R} - v_I) \end{aligned} \quad (\text{III-44})$$

$$\sigma_{r_s} - \sigma_{r_I} = -\rho_{\ell_p} (v_I - \dot{R})(v_I - v_s) \quad (\text{III-45})$$

The quantities σ_{r_I} and v_I at $r = R$ are given by Eqs. III-38, III-39. Use of Eq. III-43 enables the quantity, $g_s(t)$, in Eq. III-41 to be expressed in terms of $p(t)$.

Then, the new relationship for σ_{rs} is given by

$$\begin{aligned} \sigma_{rs} = & -p(t) + 2Y_s \ln \frac{r}{a} + 2 \int_a^r \frac{1}{r'} E_{ts} \left(2 \ln \frac{r'}{r_0} + \frac{2}{3} \bar{\epsilon}_{ls} \right) dr' \\ & + \rho_{ls} \dot{f}_s \left(\frac{1}{a} - \frac{1}{r} \right) - \frac{1}{2} \rho_{ls} f_s^2 \left(\frac{1}{a^4} - \frac{1}{r^4} \right) \end{aligned} \quad (\text{III-46})$$

From the boundary condition of Eq. III-44,

$$v_s \Big|_{r=R} = \left(1 - \frac{\rho_{lp}}{\rho_{ls}} \right) \dot{R} + \frac{\rho_{lp}}{\rho_{ls}} v_I \quad (\text{III-47})$$

Then,

$$f_s(t) = \left(1 - \frac{\rho_{lp}}{\rho_{ls}} \right) R^2 \dot{R} + \frac{\rho_{lp}}{\rho_{ls}} f_I(t) \quad (\text{III-48})$$

Substitution into the boundary condition given by Eq. III-45 yields

$$\sigma_{rs} - \sigma_{rI} \Big|_{r=R} = \rho_{lp} \left(\dot{R} - \alpha_p \frac{b^2 \dot{b}}{R^2} \right) \left(\alpha_p \frac{b^2 \dot{b}}{R^2} - \alpha_{ls} \dot{R} - (1 - \alpha_{ls}) \alpha_p \frac{b^2 \dot{b}}{R^2} \right) \quad (\text{III-49})$$

or

$$\sigma_{rs} - \sigma_{rI} \Big|_{r=R} = \rho_{lp} \left(-\alpha_{ls} \dot{R}^2 + 2\alpha_{ls} \alpha_p \frac{b^2 \dot{b} \dot{R}}{R^2} - \alpha_p^2 \alpha_{ls} \frac{b^4 \dot{b}^2}{R^4} \right) \quad (\text{III-50})$$

Substitution of Eqs. III-46, III-38 in Eq. III-50 gives

$$\begin{aligned}
 & - p(t) + 2Y_s \ln \frac{R}{a} + 2 \int_a^R \frac{1}{r'} E_{ts} \left(2 \ln \frac{r'}{r_o} + \frac{2}{3} \epsilon_{ls} \right) dr' \\
 & + \rho_{ls} \left[\alpha_{ls} (2R\dot{R}^2 + R^2\ddot{R}) + \frac{\rho_{lp}}{\rho_{ls}} \alpha_p (2b\dot{b}^2 + b^2\ddot{b}) \right] \left(\frac{1}{a} - \frac{1}{R} \right) \\
 & - \frac{1}{2} \rho_{ls} \left[\left(1 - \frac{\rho_{lp}}{\rho_{ls}} \right) R^2\dot{R} + \frac{\rho_{lp}}{\rho_{ls}} \alpha_p b^2\dot{b} \right]^2 \left(\frac{1}{a^4} - \frac{1}{R^4} \right) \\
 & + P_I + \alpha_p \rho_o \dot{b}^2 + \alpha_p \rho_{lp} (2b\dot{b}^2 + b^2\ddot{b}) \left(\frac{1}{R} - \frac{1}{b} \right) \\
 & + \frac{1}{2} \alpha_p^2 \rho_{lp} b^4 \dot{b}^2 \left(\frac{1}{R^4} - \frac{1}{b^4} \right) \\
 & = \rho_{lp} \left(- \alpha_{ls} \dot{R}^2 + 2\alpha_{ls} \alpha_p \frac{b^2 \dot{b} \ddot{R}}{R^2} - \alpha_p^2 \alpha_{ls} \frac{b^4 \dot{b}^2}{R^4} \right) \quad (III-51)
 \end{aligned}$$

where

$$\begin{aligned}
 P_I & = - \frac{2}{3} Y \ln \left(1 - e^{-3\beta} \frac{\rho_o}{\rho_{lp}} \right) + \frac{2}{27} \pi^2 E_t \\
 & - \frac{4}{9} E_t \sum_{n=1}^{\infty} \frac{1}{n^2} \left(1 - e^{-3\beta} \frac{\rho_o}{\rho_{lp}} \right) + \frac{4}{9} E \left(1 - e^{-3\beta} \right) \quad (III-52)
 \end{aligned}$$

Solving Eq. III-51 for the dynamic pressure variation at the cavity surface and subsequent rearrangement yields

$$\begin{aligned}
 p(t) = & 2Y_s \ln \frac{R}{a} + 2 \int_a^R \frac{1}{r'} E_{ts} \left(2 \ln \frac{r'}{r_o} + \frac{2}{3} \bar{\epsilon}_{ls} \right) dr' \\
 & + \alpha_{ls} \rho_{ls} (2R\dot{R}^2 + R^2\ddot{R}) \left(\frac{1}{a} - \frac{1}{R} \right) \\
 & + \alpha_p \rho_{lp} (2b\dot{b}^2 + b^2\ddot{b}) \left(\frac{1}{a} - \frac{1}{b} \right) \\
 & - \frac{1}{2} \rho_{ls} \left[\alpha_{ls} R^2 \dot{R} + \frac{\rho_{lp}}{\rho_{ls}} \alpha_p b^2 \dot{b} \right]^2 \left(\frac{1}{a^4} - \frac{1}{R^4} \right) \\
 & + \frac{1}{2} \alpha_p^2 \rho_{lp} b^4 \dot{b}^2 \left(\frac{1}{R^4} - \frac{1}{b^4} \right) + P_I \\
 & + \alpha_p \rho_o \dot{b}^2 + \alpha_{ls} \rho_{lp} \dot{R}^2 - 2\rho_{lp} \alpha_{ls} \alpha_p \frac{b^2 \dot{b}}{R^2} \dot{R} \\
 & + \alpha_p^2 \alpha_{ls} \rho_{lp} \frac{b^4 \dot{b}^2}{R^4}
 \end{aligned} \tag{III-53}$$

The following relationships have been derived in Ref. 3 and are listed for convenience.

$$2 \int_a^R \frac{1}{r'} E_{ts} \left(2 \ln \frac{r'}{r_o} + \frac{2}{3} \bar{\epsilon}_{ls} \right) dr' = \frac{2}{27} \pi^2 E_{ts} - \frac{4}{9} E_{ts} \eta \tag{III-54}$$

$$2Y_s \ln \frac{R}{a} = -\frac{2}{3} Y_s \ln \left(1 - e^{-3\beta_s \frac{\rho_{os}}{\rho_{ls}}} \right) \tag{III-55}$$

where

$$\beta_s = \frac{Y_s}{2E_s} - \frac{\bar{\epsilon}_{ls}}{3} \quad (\text{III-56})$$

$$\alpha_{ls} (2R\dot{R}^2 + R^2\ddot{R}) = 2a\dot{a}^2 + a^2\ddot{a} \quad (\text{III-57})$$

$$\alpha_{ls} R^2 \dot{R} = a^2 \dot{a} \quad (\text{III-58})$$

$$\frac{b}{R} = \left(1 - e^{-3\beta} \frac{\rho_o}{\rho_{lp}} \right)^{-1/3} \quad (\text{III-59})$$

where

$$\beta = \frac{Y}{2E} - \frac{\bar{\epsilon}_{lp}}{3} \quad (\text{III-60})$$

$$\frac{R}{a} = \left(1 - e^{-3\beta_s} \frac{\rho_{os}}{\rho_{lp}} \right)^{-1/3} \quad (\text{III-61})$$

$$(b^3 - R^3) \rho_{lp} = (b_o^3 - R_o^3) \rho_o \quad (\text{III-62})$$

$$b_o = b e^{-\beta} \quad (\text{III-63})$$

Using Eqs. III-62, III-63

$$b^3 \left(1 - e^{-3\beta} \frac{\rho_o}{\rho_{lp}} \right) = R^3 \left(1 - \frac{R_o^3}{R^3} \frac{\rho_o}{\rho_{lp}} \right) \quad (\text{III-64})$$

or

$$b = R \left(1 - e^{-3\beta} \frac{\rho_o}{\rho_{lp}} \right)^{-1/3} \left(1 - \frac{R_o^3}{R^3} \frac{\rho_o}{\rho_{lp}} \right)^{1/3} \quad (\text{III-65})$$

Now $\rho_{lp} > \rho_o$, and for deep penetration depths of the order of several projectile diameters in ice, $R^3 \gg R_o^3$. Thus, Eq. III-65 becomes

$$b \cong R \bar{\alpha}_p^{-1/3} \quad (\text{III-66})$$

where

$$\bar{\alpha}_p = \left(1 - e^{-3\beta} \frac{\rho_o}{\rho_{lp}} \right) \quad (\text{III-67})$$

It follows readily that

$$b = a \left(1 - e^{-3\beta_s} \frac{\rho_{os}}{\rho_{lp}} \right)^{-1/3} \left(1 - e^{-3\beta} \frac{\rho_o}{\rho_{lp}} \right)^{-1/3} \quad (\text{III-68})$$

or

$$b = a \bar{\alpha}_s^{-1/3} \bar{\alpha}_p^{-1/3} \quad (\text{III-69})$$

where

$$\bar{\alpha}_s = \left(1 - e^{-3\beta_s} \frac{\rho_{os}}{\rho_{lp}} \right) \quad (\text{III-70})$$

Introduction of these relationships in Eq. III-53 yields

$$\begin{aligned}
 p(t) = & -\frac{2}{3} Y_s \ln \left(1 - e^{-3\beta_s \frac{\rho_{os}}{\rho_{ls}}} \right) + \frac{2}{27} \pi^2 E_{ts} \\
 & - \frac{4}{9} E_{ts} \eta + \rho_{ls} (a^2 \ddot{a} + 2a \dot{a}^2) \left(\frac{1}{a} - \frac{1}{R} \right) \\
 & + \alpha_p \rho_{lp} (\bar{\alpha}_p)^{-1} (\bar{\alpha}_s)^{-1} (a^2 \ddot{a} + 2a \dot{a}^2) \left(\frac{1}{a} - \frac{1}{b} \right) \\
 & - \frac{1}{2} \rho_{ls} \left[a^2 \dot{a} + \frac{\rho_{lp}}{\rho_{ls}} \alpha_p (\bar{\alpha}_p)^{-1} (\bar{\alpha}_s)^{-1} a^2 \dot{a} \right]^2 \left(\frac{1}{a^4} - \frac{1}{R^4} \right) \\
 & + \frac{1}{2} \alpha_p^2 \rho_{lp} (\bar{\alpha}_p)^{-2} (\bar{\alpha}_s)^{-2} a^4 \dot{a}^2 \left(\frac{1}{R^4} - \frac{1}{b^4} \right) \\
 & + P_I + \alpha_p \rho_o (\bar{\alpha}_p)^{-2/3} (\bar{\alpha}_s)^{-2/3} \dot{a}^2 + \rho_{lp} \alpha_{ls} (\bar{\alpha}_s)^{-2/3} \dot{a}^2 \\
 & - 2\rho_{lp} \alpha_{ls} \alpha_p (\bar{\alpha}_p)^{-1} (\bar{\alpha}_s)^{-2/3} \dot{a}^2 \\
 & + \rho_{lp} \alpha_p^2 \alpha_{ls} (\bar{\alpha}_p)^{-2} (\bar{\alpha}_s)^{-2/3} \dot{a}^2
 \end{aligned} \tag{III-71}$$

Now let

$$\begin{aligned}
 P_{II} = & P_I - \frac{2}{3} Y_s \ln \left(1 - e^{-3\beta_s \frac{\rho_{os}}{\rho_{ls}}} \right) \\
 & + \frac{2}{27} \pi^2 E_{ts} - \frac{4}{9} E_{ts} \eta
 \end{aligned} \tag{III-72}$$

Then

$$\begin{aligned}
 p(t) = & P_{II} + (a\ddot{a} + 2\dot{a}^2) \left[\rho l_s \left(1 - \bar{\alpha}_s^{1/3} \right) \right. \\
 & \left. + \frac{\alpha_p \rho l_p}{\bar{\alpha}_p \bar{\alpha}_s} \left(1 - \bar{\alpha}_s^{1/3} \bar{\alpha}_p^{1/3} \right) \right] \\
 & - \frac{1}{2} \rho l_s \dot{a}^2 \left[1 + \frac{\rho l_p}{\rho l_s} \frac{\alpha_p}{\bar{\alpha}_p \bar{\alpha}_s} \right]^2 \left(1 - \bar{\alpha}_s^{4/3} \right) \\
 & + \frac{1}{2} \frac{\alpha_p^2 \rho l_p}{\bar{\alpha}_p^2 \bar{\alpha}_s^2} \left(1 - \bar{\alpha}_s^{4/3} \right) \dot{a}^2 \\
 & + \dot{a}^2 \left[\frac{\alpha_p \rho}{\bar{\alpha}_p^{2/3} \bar{\alpha}_s^{2/3}} + \frac{\alpha l_s \rho l_p}{\bar{\alpha}_s^{2/3}} - 2\rho l_p \frac{\alpha l_s \alpha_p}{\bar{\alpha}_p \bar{\alpha}_s^{2/3}} + \frac{\alpha_p^2 \alpha l_s}{\bar{\alpha}_p^2 \bar{\alpha}_s^{2/3}} \rho l_p \right] \quad (III-73)
 \end{aligned}$$

Rearranging

$$\begin{aligned}
 p(t) = & P_{II} + a\ddot{a} \left[\rho l_s \left(1 - \bar{\alpha}_s^{1/3} \right) + \frac{\alpha_p \rho l_p}{\bar{\alpha}_p \bar{\alpha}_s} \left(1 - \bar{\alpha}_s^{1/3} \bar{\alpha}_p^{1/3} \right) \right] \\
 & + \dot{a}^2 \left[2\rho l_s \left(1 - \bar{\alpha}_s^{1/3} \right) + \frac{2\alpha_p \rho l_p}{\bar{\alpha}_p \bar{\alpha}_s} \left(1 - \bar{\alpha}_s^{1/3} \bar{\alpha}_p^{1/3} \right) \right. \\
 & - \frac{1}{2} \rho l_s \left(1 + \frac{\rho l_p}{\rho l_s} \frac{\alpha_p}{\bar{\alpha}_p \bar{\alpha}_s} \right)^2 \left(1 - \bar{\alpha}_s^{4/3} \right) \\
 & + \frac{1}{2} \frac{\alpha_p^2 \rho l_p}{\bar{\alpha}_p^2 \bar{\alpha}_s^2} \left(1 - \bar{\alpha}_s^{4/3} \right) + \frac{\alpha_p \rho}{\bar{\alpha}_p^{2/3} \bar{\alpha}_s^{2/3}} + \frac{\alpha l_s \rho l_p}{\bar{\alpha}_s^{2/3}} \\
 & \left. - 2\rho l_p \frac{\alpha l_s \alpha_p}{\bar{\alpha}_p \bar{\alpha}_s^{2/3}} + \frac{\alpha_p^2 \alpha l_s}{\bar{\alpha}_p^2 \bar{\alpha}_s^{2/3}} \rho l_p \right] \quad (III-74)
 \end{aligned}$$

Equation III-74 can be rewritten as

$$p(t) = P_{II} + C_1 \ddot{a} + C_2 \dot{a}^2 \quad (\text{III-75})$$

where

$$C_1 = \rho l_s \left(1 - \alpha_s^{1/3}\right) + \frac{\alpha_p \rho l_p}{\bar{\alpha}_p \bar{\alpha}_s} \left(1 - \bar{\alpha}_s^{1/3} \bar{\alpha}_p^{1/3}\right) \quad (\text{III-76})$$

$$\begin{aligned} C_2 = & 2\rho l_s \left(1 - \bar{\alpha}_s^{1/3}\right) + 2 \frac{\alpha_p \rho l_p}{\bar{\alpha}_s \bar{\alpha}_p} \left(1 - \bar{\alpha}_s^{1/3} \bar{\alpha}_p^{1/3}\right) \\ & - \frac{1}{2} \rho l_s \left(1 + \frac{\rho l_p}{\rho l_s} \frac{\alpha_p}{\bar{\alpha}_p \bar{\alpha}_s}\right)^2 \left(1 - \bar{\alpha}_s^{4/3}\right) \\ & + \frac{1}{2} \frac{\rho l_p \alpha_p^2}{\bar{\alpha}_p^2 \bar{\alpha}_s^2} \left(1 - \bar{\alpha}_s^{4/3}\right) + \frac{\alpha_p \rho}{\bar{\alpha}_p^{2/3} \bar{\alpha}_s^{2/3}} + \frac{\alpha_s \rho l_p}{\bar{\alpha}_s^{2/3}} \\ & - 2\rho l_p \frac{\alpha_s \alpha_p}{\bar{\alpha}_p \bar{\alpha}_s^{2/3}} + \frac{\alpha_p^2 \alpha_s}{\bar{\alpha}_p^2 \bar{\alpha}_s^{2/3}} \rho l_p \end{aligned} \quad (\text{III-77})$$

It has been shown in Ref. 3 that an expression for dynamic pressure at the spherical cavity surface, such as the one given by Eq. III-75, can be employed to derive an equation of motion for projectile penetration. In the present case, the following relationship is obtained

$$M\ddot{q} = - \left[P_{II} + \frac{2}{3} \left(C_1 \frac{D}{2} \ddot{q} + C_2 \dot{q}^2 \right) \right] \frac{\pi D^2}{4} \quad (\text{III-78})$$

The usual process of integration yields

$$\ln \frac{P_{II} + 2/3 C_1 \dot{q}^2}{P_{II} + 2/3 C_2 v_{os}^2} = - \frac{4 C_2 (q - q_{os})}{3 M/A + C_1 D/3} \quad (III-79)$$

Solving for the terminal penetration depth

$$q_t = q_{os} + \frac{3}{4} \frac{M/A + C_1 D/3}{C_2} \ln \frac{P_{II} + 2/3 C_2 v_{os}^2}{P_{II}} \quad (III-80)$$

Here, q_{os} and v_{os} refer to the penetration depth and exit velocity, respectively, characterizing projectile transit through the overlying snow cover. These quantities are obtained from solution of the first phase penetration problem.

Appendix A

LISTING FOR LARGE DEFORMATION THEORY COMPUTER CODE
THAT INCORPORATES STRESS REDISTRIBUTIONS DUE TO FRACTURE

Preceding page blank

```
//LISTER JOB 'A519***,602,1,9','SIOHU'
//*SERVICE LIST
//*PRINT COPIES=2
//STPPL EXEC FORTHCLG
//FORT,SYSIN CD *
```

```
C *****
```

```
C
C   VERSION FSP1....TWO DIMENSIONAL AXISYMMETTRIC 'CANDIA' CODE.
C   THIS VERSION COMPATIBLE ON ANY IBM 360 MACHINE
C   LANGUAGE....FORTRAN (IV) H
```

```
C *****
```

```
IMPLICIT REAL*8 (A-H,O-Z,S), INTEGER (I-N)
COMMON /CCM1/ AR (24,46), ARH (24,46), ARDH(24,46),
1  AZ (24,46), AZH (24,46), AZDH(24,46),
2  AA (24,46), AV (24,46), AP (24,46),
3  ATRP(24,46), ATZZ(24,46), ATRZ(24,46),
4  ATTT(24,46),
5  ASRR(24,46), ASZZ(24,46), ASRZ(24,46),
6  ASTT(24,46)
COMMON /CCM2/ BR (46, 6), BRH (46, 6), BRDH(46, 6),
1  BZ (46, 6), BZH (46, 6), BZDH(46, 6),
2  BA (46, 6), BV (46, 6), BP(46, 6),
3  BTRP(46, 6), BTZZ(46, 6), BTRZ(46, 6),
4  BTTT(46, 6),
5  BSRR(46, 6), BSZZ(46, 6), BSZR(46, 6),
6  BSTT(46, 6)
COMMON /CCM3/ TR (24,46), TRH (24,46), TRDH(24,46),
1  T7 (24,46), TZH (24,46), TZDH(24,46),
2  SR(46), SZ(46), TSR(46), TSZ(46), ZM(2,46), SPTM(5),
4  A1(2), A2(2), A3(2), A4(2), ALEN(2), AMAT(2), ANU(2), AVU(2),
5  BK(2), CAPE(2), CDUT(2), DR(2), D7(2), RAD(2), RHO(2), RDOT(2),
6  RHOG(2), PHCT(2), TWNU(2), YT(2), ZDUT(2), ZV(2), VCUN(2),
7  CQ,DTH,DTHW,DTHW,ZDINT,TYMF,CHEKO,FACTP
COMMON /ICCM1/ IPTA(24,46)
COMMON /ICCM2/ IPTB(46, 6)
COMMON /ICCM3/ ISHP(2), JM(2), KM(2), KMID,
1  IPUN,ICT1,ICT2,IDENT,IMAX,IPRNT,ICVCL,IMAP,NTT,KINT,KMN,KMX
```

```
C *****
C   SFT ARTIFICIAL VISCOSITY COEFFICIENT VALUE
```

```
C *****
C   CQ=0.7
C   READ (5,100) IDENT
C   100 FORMAT (I10)
```

```
C *****
C   IDENT = 1 NEW RUN NO SAVE
C           = 2 NEW RUN SAVE
C           = 3 RESUME NO SAVE
C           = 4 RESUME SAVE
```

```
C *****
C   IF (IDENT.CF.3) CALL RSME
C   IF (IDENT.CF.3) GO TO 300
```

NOT REPRODUCIBLE

```

C *****
C
C      READ IN DATA FROM CARDS
C
C *****
C      CALL INPTT
C *****
C
C      DO ALL INITIAL MODIFICATION OF DATA...UNITS ETC
C
C *****
C      CALL INITT
C *****
C
C      CREATE THE FINITE DIFFERENCE GRID WORK AND ALL DISC FILES
C
C *****
C      CALL GRIDC
C *****
C
C      WRITE OUT THE SALIENT ASPECTS OF THE PROBLEM
C
C *****
C      300 CALL INWRR
C *****
C
C      CYCLE THROUGH THE BODY IS INITIATED
C
C *****
C      300 CALL LETGC
C *****
C
C      DO ALL NECESSARY COMPUTATION FOR THE TARGET
C
C *****
C      CALL      GUTT ( 1,IPTA,AR,AZ,ARH,AZH,ARDH,AZDH,ATRR,ATZZ,ATRZ,
1                ATTT,ASRR,ASZZ,ASRZ,ASTT,AA,AV,AP,KMID,KMY,KINT,
2                JMX)
C *****
C
C      BEFORE GOING TO THE PROJECTILE DO ALL PREPARATIONS NECESSARY
C
C *****
C      JJJ=JM(2)
C      DO 304 J=1,JJJ
C      BRH(1,J) = ARH(KINT,J)
C      BZH(1,J) = AZH(KINT,J)
C      BRDH(1,J) = ARDH(KINT,J)
C      304 BZDH(1,J) = AZDH(KINT,J)
C *****
C
C      NOW DO ALL THE COMPUTATIONS FOR THE PROJECTILE
C
C *****
C      K2 = KM(2)
C      CALL      GUTT ( 2,IPTB,BR,BZ,BRH,BZH,BRDH,BZDH,BTRR,BTZZ,BTRZ,
1                HTTT,HSRR,HSZZ,HSRZ,HSTT,BA,BV,HP,K2, 2,KMY,
2                JM(2) )
C *****
C

```



```

C      CHECK IF IT IS TIME TO QUIT
C
C      *****
      IF (ICVCL-IMAX) 300,301,301
301 IF ((IDENT.EQ.2).OR.(IDENT.EQ.4)) CALL SSAV
      RETURN
      END
      SUBROUTINE PSNF
      IMPLICIT REAL*4 (A-H,O-Z,S), INTEGER (I-N)
      COMMON /CCM1/ AR (24,46), APH (24,46), ARDH(24,46),
1      AZ (24,46), AZH (24,46), AZDH(24,46),
2      AA (24,46), AV (24,46), AP (24,46),
3      ATPR(24,46), ATZZ(24,46), ATRZ(24,46),
4      ATTT(24,46),
5      ASPR(24,46), ASZZ(24,46), ASRZ(24,46),
6      ASTT(24,46)
      COMMON /CCM2/ RH (46,6), RPH (46,6), RRDH(46,6),
1      RZ (46,6), RZH (46,6), RZDH(46,6),
2      RA (46,6), RV (46,6), RP(46,6),
3      RTRR(46,6), RTZZ(46,6), RTRZ(46,6),
4      RTTT(46,6),
5      RSRR(46,6), RSZZ(46,6), RSRZ(46,6),
6      RSTT(46,6)
      COMMON /CCM3/ TR (24,46), TRH (24,46), TRDH(24,46),
1      TZ (24,46), TZH (24,46), TZDH(24,46),
2      SR(46), SZ(46), TSR(46), TSZ(46), ZM(2,46), SPTM(5),
3      AI(2), A2(2), A3(2), A4(2), ALEN(2), AMAT(2), AMH(2), ANU(2),
4      AK(2), CAPE(2), COUT(2), DR(2), JZ(2), RAD(2), RHO(2), RDOT(2),
5      RHUG(2), RHOT(2), TWMU(2), YT(2), ZDOT(2), ZV(2), VCON(2),
6      CQ,DTH,CTH,DTHW,DTMIN,ZDINT,TYMF,CHEKD,FACTR
      COMMON /ICCM1/ IPTA(24,46)
      COMMON /ICCM2/ IPTH(46,6)
      COMMON /ICCM3/ ISHP(2), JM(2), KM(2), KMID,
1      IRUN,ICT1,IUT2,IDENT,IMAX,IPRNT,ICVCL,IMAP,NTT,KINT,KMN,KMY
      RETURN
      END
      SUBROUTINE SSAV
      IMPLICIT REAL*4 (A-H,O-Z,S), INTEGER (I-N)
      COMMON /CCM1/ AR (24,46), APH (24,46), ARDH(24,46),
1      AZ (24,46), AZH (24,46), AZDH(24,46),
2      AA (24,46), AV (24,46), AP (24,46),
3      ATPR(24,46), ATZZ(24,46), ATRZ(24,46),
4      ATTT(24,46),
5      ASPR(24,46), ASZZ(24,46), ASRZ(24,46),
6      ASTT(24,46)
      COMMON /CCM2/ RH (46,6), RPH (46,6), RRDH(46,6),
1      RZ (46,6), RZH (46,6), RZDH(46,6),
2      RA (46,6), RV (46,6), RP(46,6),
3      RTRR(46,6), RTZZ(46,6), RTRZ(46,6),
4      RTTT(46,6),
5      RSRR(46,6), RSZZ(46,6), RSRZ(46,6),
6      RSTT(46,6)
      COMMON /CCM3/ TR (24,46), TRH (24,46), TRDH(24,46),
1      TZ (24,46), TZH (24,46), TZDH(24,46),
2      SR(46), SZ(46), TSR(46), TSZ(46), ZM(2,46), SPTM(5),
3      AI(2), A2(2), A3(2), A4(2), ALEN(2), AMAT(2), AMH(2), ANU(2),
4      AK(2), CAPE(2), COUT(2), DR(2), JZ(2), RAD(2), RHO(2), RDOT(2),
5      RHUG(2), RHOT(2), TWMU(2), YT(2), ZDOT(2), ZV(2), VCON(2),
6      CQ,DTH,CTH,DTHW,DTMIN,ZDINT,TYMF,CHEKD,FACTR
      COMMON /ICCM1/ IPTA(24,46)

```

NOT REPRODUCIBLE

```

COMMON /ICOM2/ IPTB(46, 6)
COMMON /ICCM3/ ISHP(2), JM(2), KM(2),      KMID,
1 IRUN, IDT1, IDT2, IDENT, IMAX, IPRNT, ICYCL, IMAP, NTT, KINT, KMN, KMX
RETURN
END
SUBROUTINE INPTT
  IMPLICIT REAL*8 (A-H,O-Z,S), INTEGER (I-N)
  COMMON /CCM1/ AR (24,46), ARH (24,46), ARDH(24,46),
1  AZ (24,46), AZH (24,46), AZDH(24,46),
2  AA (24,46), AV (24,46), AP (24,46),
3  ATRR(24,46), ATZZ(24,46), ATRZ(24,46),
4  ATTT(24,46),
5  ASRP(24,46), ASZZ(24,46), ASRZ(24,46),
6  ASTT(24,46)
  COMMON /CCM2/ BR (46, 6), BRH (46, 6), BRDH(46, 6),
1  BZ (46, 6), BZH (46, 6), BZDH(46, 6),
2  BA (46, 6), BV (46, 6), BP(46, 6),
3  BTRR(46, 6), BTZZ(46, 6), BTRZ(46, 6),
4  BTTT(46, 6),
5  BSPR(46, 6), BSZZ(46, 6), BSRZ(46, 6),
6  BSTT(46, 6)
  COMMON /CCM3/ TR (24,46), TRH (24,46), TRDH(24,46),
1  TZ (24,46), TZH (24,46), TZDH(24,46),
2  SR(46), SZ(46), TSR(46), TSZ(46), ZM(2,46), SPTM(5),
4  A1(2), A2(2), A3(2), A4(2), ALEN(2), AMAT(2), AMU(2), ANU(2),
5  BK(2), CAPF(2), CDDT(2), DR(2), DZ(2), RAD(2), RHO(2), RDOT(2),
6  RHUG(2), RHOT(2), TWMU(2), YT(2), ZDDT(2), ZV(2), VCON(2),
7  CQ,DTN,CTH,DTW,DTMIN,ZDINT,TYME,CHEKD,FACTR
  COMMON /ICCM1/ IPTA(24,46)
  COMMON /ICCM2/ IPTB(46, 6)
  COMMON /ICCM3/ ISHP(2), JM(2), KM(2),      KMID,
1 IRUN, IDT1, IDT2, IDENT, IMAX, IPRNT, ICYCL, IMAP, NTT, KINT, KMN, KMX
  NCR=5

```

```

C * *****
C
C  READ IDENTIFIERS:
C
C    IRUN : RUN I.D. NO
C    IDT1 : MONTH-DAY (EG. 1103 - 3RD NOV)
C    IDT2 : YEAR      (EG. 69 - FOR 1969)
C    FACTR : FRACTION OF DIAGONAL USED TO FIND THE TIME STEP
C
C *****
C    READ (NCR,100) IRUN, IDT1, IDT2, FACTR
C *****
C
C  READ CONTROL VARIABLES
C
C    IMAX - MAXIMUM NO. OF CYCLES BEFORE PROBLEM TERMINATION
C    IPRNT - MAXIMUM NO. OF CYCLES BETWEEN PRINTOUTS
C    IMAP - MAXIMUM NO. OF CYCLES BETWEEN GRAPHICAL OUTPUTS
C    NTT - NO. OF SPECIAL PRINT TIMES
C    SPTM(NTT) SPECIAL PRINT TIMES IN MICRO-SECONDS
C
C *****
C    READ (NCR,101) IMAX, IPRNT, IMAP, NTT
C    READ (NCR,102) (SPTM(K), K=1,NTT)
C *****
C
C  READ MATERIAL PROPERTIES

```



```

2  SR(46), SZ(46), TSR(46), TSZ(46), ZM(2,46), SPTH(5),
4  A1(2), A2(2), A3(2), A4(2), ALEN(2), AMAT(2), AMU(2), ANU(2),
5  BK(2), CAPE(2), CDCT(2), DR(2), DZ(2), RAD(2), RHO(2), ROOT(2),
6  RHOG(2), RHOT(2), TWMU(2), YT(2), ZDCT(2), ZV(2), VCON(2),
7  CQ,DTH,DTHW,DTMIN,ZDINT,TYME,CHFKD,FACTR
COMMON /ICOM1/ IPTA(24,46)
COMMON /ICOM2/ IPTB(46, 6)
COMMON /ICOM3/ ISHP(2), JM(2), KM(2), KMD,
1  IRUN, IDT1, IDT2, IDENT, IMAX, IPRNT, ICYCL, IMAP, INT, KINT, KMN, KMX
DO 301 J=1,2
  RHUG(J)= RHO(J)
  RHO(J) = 9.35432D-05 * RHOG(J)
C *****
C
C NOW RHUG IS IN (GM/CC)
C PHU IS IN (LB-SFG2/IN4)
C
C *****
  AMU(J)= (CAPE(J)*0.5)/(1.0+ANU(J))
  BK(J) = CAPE(J)/(3.0*(1.0-2.0*AMU(J)))
  CDCT(J)=DSQRT((BK(J)+4.0*AMU(J)/3.0)/RHO(J))*1.0D-06
  VCON(J)= CDCT(J)/1.2D-05
C *****
C
C UNITS: AMU,BK ARE IN (PSI)
C CDCT IS IN (INCHES PER MICROSEC)
C VCON IS IN (FEET PER SEC)
C
C *****
  ALEN(J) = DZ(J) * KM(J)
  RAD(J) = DP(J) * JM(J)
C *****
C NOW CHANGE JM AND KM TO STAND FOR NO OF GRID ROWS AND COL MNS
C INSTEAD OF NO OF GRID CELLS
C *****
  JM(J) = JM(J) + 1
  KM(J) = KM(J) + 1
  ZV(J) = ZDCT(J)
  ZDCT(J) = 12.0D-06 * ZDCT(J)
C *****
C UNITS: ZV IS IN (FT/SEC)
C ZDCT IS IN (INCH PER MICROSEC)
C *****
C
C NEXT COMPUTE VALUES FOR TIME STEP IN MICROSEC
C
  DTHW = FACTR*DSQRT(DR(J)**2 + DZ(J)**2)/CDCT(J)
C *****
  IF (J-1) 300,300,301
300 DTH=DTHW
301 CONTINUE
C *****
C NOW SELECT THE SMALLER OF DTH & DTHW TO BE THE TIME STEP
C *****
  IF (DTH-DTHW) 303,303,302
302 DTH=DTHW
303 DTMIN = DTH * 0.1
  KINT = KM(J)
  KMD = KINT + 1

```

```

C *****
C-- COMPUTE THE INTERFACE VELOCITY
C *****
      ZDINT= (ZDOT(1)*RHO(1)*CDO(1) + ZDOT(2)*RHO(2)*CDO(2))/(RHO(1)*
1      CDO(1) + RHO(2)*CDO(2))
      RETURN
      END
      SUBROUTINE INWR
      IMPLICIT REAL*8 (A-H,C-Z,*), INTEGER (I-N)
      COMMON /CCM1/ AR (24,46), ARH (24,46), ARDH(24,46),
1      AZ (24,46), AZH (24,46), AZDH(24,46),
2      AA (24,46), AV (24,46), AP (24,46),
3      ATPR(24,46), ATZ(24,46), ATPZ(24,46),
4      ATTT(24,46),
5      ASRR(24,46), ASZ(24,46), ASRZ(24,46),
6      ASTT(24,46)
      COMMON /CCM2/ BR (46, 6), BRH (46, 6), BRDH(46, 6),
1      BZ (46, 6), BZH (46, 6), BZDH(46, 6),
2      BA (46, 6), BV (46, 6), BP(46, 6),
3      BTRF(46, 6), BTZ(46, 6), BTRZ(46, 6),
4      BTTT(46, 6),
5      BSRR(46, 6), BSZ(46, 6), BSRZ(46, 6),
6      BSTT(46, 6)
      COMMON /CCM3/ TR (24,46), TRH (24,46), TRDH(24,46),
1      TZ (24,46), TZH (24,46), TZDH(24,46),
2      SR(46), SZ(46), TSR(46), TSZ(46), ZM(2,46), SPTM(5),
3      A1(2), A2(2), A3(2), A4(2), ALEN(2), AMAT(2), AMU(2), AMH(2),
4      BK(2), CAPE(2), CDO(2), DR(2), DZ(2), RAD(2), RHO(2), ROOT(2),
5      RHUG(2), RHCT(2), TMM(2), YT(2), ZDOT(2), ZV(2), VCON(2),
6      CR,DTN,CTH,DTL,DTMIN,ZDINT,TYMF,CHEKD,FACTR
      COMMON /ICCM1/ IPTA(24,46)
      COMMON /ICCM2/ IPTH(46, 6)
      COMMON /ICCM3/ ISPD(2), JM(2), KM(2), KMID,
1      IRUN,INT1,INT2,IDENT,IMAX,IPRNT,ICYCL,IMAP,NTT,KINT,KMN,KMX
      NPR=6
C *****
C
C WRITE PROBLEM IDENTIFICATION
C
C *****
      WRITE (NPR,200) IRUN,INT1,INT2,IDENT
C *****
C
C WRITE MATERIAL PROPERTIES
C
C *****
      WRITE (NPR,201) AMAT(1),AMAT(2),RHUG(1),RHUG(2),RHO(1),RHO(2)
      WRITE (NPR,202) AMU(1),AMU(2),CAPE(1),CAPE(2),AMU(1),AMU(2)
      WRITE (NPR,203) BK(1),BK(2),CDO(1),CDO(2),VCON(1),VCON(2)
      WRITE (NPR,204) YT(1),YT(2),A1(1),A1(2)
C *****
C
C GEOMETRIC PROPERTIES
C
C *****
      WRITE (NPR,205) ALEN(1),ALEN(2),RAD(1),RAD(2),DR(1),DR(2)
      WRITE (NPR,206) DZ(1),DZ(2),KM(1),KM(2),JM(1),JM(2)
      WRITE (NPR,207) ROOT(1),ROOT(2),ZDOT(1),ZDOT(2),ZV(1),ZV(2)
C *****
C

```

NOT REPRODUCIBLE

```

C CONTROL DATA
C
C *****
      WRITE (NPR,208) FAC,TR,IMAX,IMAP,IPRNT,NTT
      WRITE (NPR,209) (SPTM(KKT),KKT=1,NTT)
C *****
C
C FCRMATS
C
C *****
200 FORMAT ('1',70X,'TWO-D LAGRANGIAN COMPUTATION',/,71X,'RUN. NO ',
S 14,' DATE = ',14,' ',19'12,10X,'RESUME CODE ',14,
S 'BODY B',/,)
S '////,40X,'UNITS',29X,'BODY A',14X,
201 FORMAT (2X,'MATERIAL PROPERTIES',/,5X,'MATERIAL',63X,A4,16X,A4,
S //,5X,'DENSITY (RHO)',22X,'G/CC',15X,2D20.6,/,40X,'LB-SEC2/IN4',
S 9X,2E20.6,/)
202 FORMAT (5X,21HPOISSON'S RATIO (ANU), 34X,2D20.6,/,5X,22HYOUNG'S M
SODULUS (CAPE),13X,'PSI',17X,2D20.6,/,5X,'RIGIDITY MODULUS (AMU)',
S 13X,'PSI',17X,2D20.6,/)
203 FORMAT (5X,'BULK MODULUS (BK)',18X,'PSI',17X,2D20.6,/,5X,
S 'SOUND SPEED (CDOT)',17X,'IN/MICRO-SEC',8X,
S 2D20.6,/,40X,'FT/SEC',
S 14X,2D20.6,/)
204 FORMAT (5X,'YIELD STRENGTH (YT)',16X,'PSI',17X,2D20.6,/,
S 5X,'SHEAR STRENGTH (ST)',16X,'PSI',17X,2D20.6,/)
205 FORMAT (2X,'GEOMETRIC PROPERTIES',/,5X,'LENGTH (AL EN)',22X,'INCH',
S 16X,2D20.6,/,5X,'RADIUS (RAD)',23X,'INCH',16X,2D20.6,/,5X,
S 'DR',33X,'INCH',16X,2D20.6,/)
206 FORMAT (5X,'DZ',33X,'INCH',16X,2D20.6,/,5X,'GRID POINTS Z (KM)',
S 37X,2I20,/,5X,'GRID POINTS R (JM)',37X,2I20,/)
207 FORMAT (5X,'ROCK',31X,'FT/SEC',14X,2D20.6,/,5X,'ZDOT',31X,
S 'IN/MICRO-SEC',8X,2D20.6,/,40X,'FT/SEC',14X,2D20.6,/,2X,
S 'CCNTRCL DATA',/)
208 FORMAT ('C',4X,'TIME STEP FACTOR',18X,F10.5//5X,'MAX NO OF CYCLES',
S 18X,110//5X,'MAP FREQUENCY',21X,110//5X,'PRINT FREQUENCY',19X,
S 2 110//5X,'NO OF SPECIAL PRINTS',14X,110//5X,'SPECIAL PRINT TIMES',
S 3 IN MICRO-SEC',5X)
209 FORMAT (5F15.5)
      RETURN
      END
      SUBROUTINE GRIDC
      IMPLICIT REAL*8 (A-H,C-Z,S), INTEGER (I-N)
      COMMON /CCM1/ AR (24,46), ARH (24,46), ARDH(24,46),
1 AZ (24,46), AZH (24,46), AZDH(24,46),
2 AA (24,46), AV (24,46), AP (24,46),
3 ATPR(24,46), ATZZ(24,46), ATRZ(24,46),
4 ATTT(24,46),
5 ASRR(24,46), ASZZ(24,46), ASRZ(24,46),
6 ASTT(24,46)
      COMMON /CCM2/ BR (46,6), BRH (46,6), BRDH(46,6),
1 BZ (46,6), BZH (46,6), BZDH(46,6),
2 BA (46,6), BV (46,6), BP(46,6),
3 BTRR(46,6), BTZZ(46,6), BTRZ(46,6),
4 BITT(46,6),
5 BSRR(46,6), BSZZ(46,6), BSRZ(46,6),
6 BSTT(46,6)
      COMMON /CCM3/ TR (24,46), TRH (24,46), TRDH(24,46),
1 TZ (24,46), TZH (24,46), TZDH(24,46),
2 SR(46), SZ(46), TSR(46), TSZ(46), ZM(2,46), SPTM(5),

```

```

4 A1(2), A2(2), A3(2), A4(2), ALFN(2), AMAT(2), AMU(2), AMU(2),
5 BK(2), CAPE(2), CDOT(2), CR(2), DZ(2), RAD(2), PHO(2), RHOT(2),
6 RHOG(2), RHOT(2), TWMU(2), YT(2), ZDOT(2), ZV(2), VCON(2),
7 CQ,DTN,CTH,OTHH,OTMIA,ZDINT,TYMF,CHEKD,FACTR
COMMON /ICCM1/ IPTA(24,46)
COMMON /ICCM2/ IPTB(46, 6)
COMMON /ICCM3/ ISHP(2), JM(2), KM(2), KMID,
1 IRUN,IC1,IDT2,ICENT,IMAX,IPRNT,ICYCL,IMAP,NTT,KINT,KYN,KMX
DIMENSION AREA(2), ARHC(2)
NPR=0
ON 300 I=1,2
C *****
C I=1 IS THE TARGET
C I=2 IS THE PROJECTILE
C
C AREA IS THE INITIAL AREA OF EACH CELL IN SQUARE INCHES
C ARHU IS THE PRODUCT AREA * DENSITY IN (LB-MICROSEC-2/IN-2)
C RHUT IS ONE-THIRD RHO IN LB MICROSEC INCH UNITS
C TWMU IS TWICE THE RIGIDITY MODULUS AMU.
C *****
C AREA(I)= CR(I) * DZ(I)
C ARHU(I)= AREA(I) * RHG(I) * 1.0D12
C RHUT(I)= RHO(I)/3.0D-12
C TWMU(I)= 2.0 * AMU(I)
300 CONTINUE
C *****
C
C NOW GRID IS CREATED FOR BODY 1
C *****
C ZCUR = 0.0
C JJJ = JM(1)
C JJ2 = JM(2)
C KKK = KM(1)
C DO 7777 K=1,KKK
C DO 7777 J=1,JJJ
7777 IPTA(K,J)=0
C DO 326 K=1,KKK
C RCUR = 0.0
C DO 325 J=1,JJJ
C AR (K,J) = RCUR
C AZ (K,J) = ZCUR
C ARH (K,J) = RCUR
C AZH (K,J) = ZCUR
C ARDH(K,J) = RDOT(1)
C AZDH(K,J) = ZDOT(1)
C IF (J-1) 304,304,302
302 IF (K-1) 304,304,303
303 AA(K,J)=AREA(1)
C AV(K,J)=1.0
C AP(K,J)=0.0
C ATRR(K,J)=0.0
C ATZZ(K,J)=0.0
C ATRZ(K,J)=0.0
C ATTT(K,J)=0.0
C ASRR(K,J)=0.0
C ASZZ(K,J)=0.0
C ASRZ(K,J)=0.0
C ASTT(K,J)=0.0

```

```

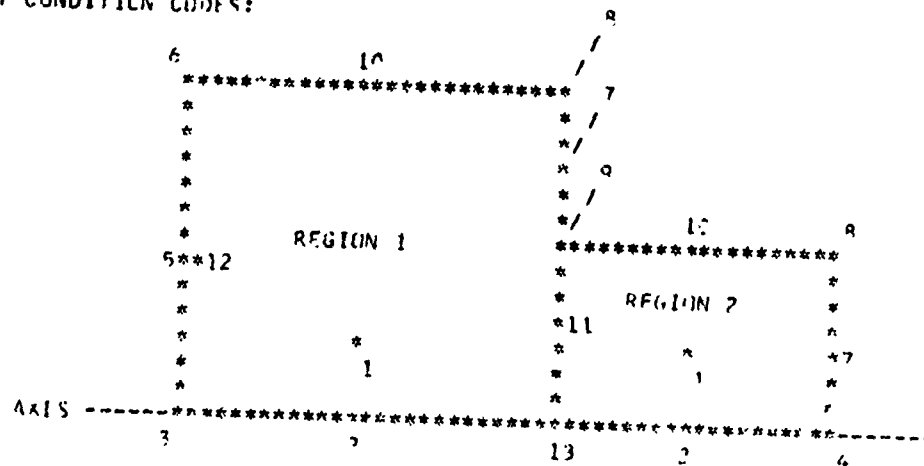
C *****
C NOW THE POINT CONDITION CODE IS DETERMINED
C *****

```

```

C POINT CONDITION CODES:

```



```

C *****
304 IF (J-1) 305,305,310
305 IF (K-1) 306,306,307
306 IP=3
GO TO 324
307 IF (K-KKK) 309,309,309
308 IP = 13
AZDH(K,J)=ZDIAT
GO TO 324
309 IP=2
GO TO 324
310 IF (K-1) 311,311,314
311 IF (J-JJJ) 312,312,312
312 IP = 6
GO TO 324
313 IP = 5
IPTA(K+1,J)=12
GO TO 324
314 IF (K-KKK) 315,315,315
315 IF (J-JJJ) 316,316,316
316 IF (JJJ-JJ2) 317,317,317
317 IP=10
AZDH(K,J)=ZDIAT
GO TO 324
318 IP=8
GO TO 324
319 IF (J-JJ2) 319,319,320
319 IP = 9
AZDH(K,J)=ZDIAT
GO TO 324

```



```

319 IP = 11
  AZDH(K,J)=ZDIAT
  GO TO 324
320 IP = 7
  GO TO 324
321 IF (J-JJJ) 323,322,322
322 IP = 10
  GO TO 324
323 IP = 1
324 IF (IPTA(K,J).EQ.0) IPTA(K,J)=IP
  RCUR = RCUR + DR(1)
325 CONTINUE
  WRITE (NPR,7000) K,(IP(A(K,KK)), KK=1,JJJ)
  ZCUR = ZCUR + DZ(1)
324 CONTINUE
C*****
C  NOW COMPUTE CELL PSEUDO-MASS ZM
C*****
  DO 400 J= 2,1JJ
    TEMP=AP(1,J)
    400 ZM(1,J) =ARH0(1)*(TEMP -0.5*DR(1))
C *****
C
C  NOW GRID FOR BODY 2 IS CREATED
C
C *****
  ZCUR = ZCUR - DZ(1)
  KKK = KM(2)
  JJJ = JM(2)
  DO 349 K=1,KKK
    RCUR =0.0
    DO 348 J=1,JJJ
      BR (K,J) = RCUR
      BZ (K,J) = ZCUR
      BRH (K,J) = RCUR
      BZH (K,J) = ZCUR
      BRDH(K,J) = RDLT(2)
      BZDH(K,J) = ZDNT(2)
      IF (J-1) 330,330,328
329 IF (K-1) 330,330,329
329 BA(K,J)=AREA(2)
      BV(K,J) = 1.0
      BP(K,J)=0.0
      BTRP(K,J)=0.0
      BTZT(K,J)=0.0
      BTRZ(K,J)=0.0
      BTTT(K,J)=0.0
      BSRR(K,J)=0.0
      BSZZ(K,J)=0.0
      BSRZ(K,J)=0.0
      BSTT(K,J)=0.0
C *****
C  NOW THE POINT CONDITION CODE IS DETERMINED
C *****
330 IF (J-1) 331,331,336
331 IF (K-1) 332,332,333
332 IP = 13
  BZDH(K,J)=ZDIAT
  GO TO 347
333 IF (K-KKK) 335,334,334

```

```

334 IP = 4
GO TO 347
335 IP = 2
GO TO 347
336 IF (K-1) 337,337,340
337 IF (J-JJJ) 339,338,338
338 IF (JJ-J*(1)) 340,339,340
339 IP=10
RZDH(K,J)=ZDINT
GO TO 347
340 IP=9
RZDH(K,J)=ZDINT
GO TO 347
339 IP=11
RZDH(K,J)=ZDINT
GO TO 347
340 IF (K-KKK) 344,341,341
341 IF (J-JJJ) 343,342,342
342 IP = 8
GO TO 347
343 IP = 7
GO TO 347
344 IF (J-JJJ) 346,345,345
345 IP = 10
GO TO 347
346 IP = 1
347 IPTB(K,J)=IP
RCUR = RCUR +DR(2)
349 CONTINUE
WRITE (NPR,7000) K,(IPTB(K,KK),KK=1,JJJ)
ZCUR = ZCUR +DZ(2)
349 CONTINUE
C *****
C NOW COMPUTE CELL PSEUDO-MASS ZM
C *****
      DN 401 J=2,JJJ
      TEMP=BR(1,J)
401 ZM(2,J) = ARHG(2) * (TEMP -0.5*DR(2))
C *****
C
C INITIALISE CYCLE COUNTER, TIME, TIME STEPS,WAVE BOUNDARIES
C
C *****
      ICYCL =0
      TYME =0
      DTN =DTF
      DTHW =DTH
      KMN =KINT -3
      KMX = 4
      JMX = JM(2) + 2
      IF (JMX.GT.JM(1)) JMX=JM(1)
7000 FORMAT ('C',20I5)
      RETURN
      END
      SUBROUTINE LETGC
      IMPLICIT REAL*8 (A-H,C-Z,S), INTEGER (I-N)
      COMMON /CCM1/ AR (24,46), ARH (24,46), ARDH(24,46),
1          AZ (24,46), AZH (24,46), AZDH(24,46),
2          AA (24,46), AV (24,46), AP (24,46),
3          ATRR(24,46), ATZZ(24,46), ATRZ(24,46),

```

```

4          ATTT(24,46),
5          ASPR(24,46), ASZ7(24,46), ASR7(24,46),
6          ASTT(24,46)
COMMON /CCP2/ BR (46, 6), BRH (46, 6), BRDH(46, 6),
1          BZ (46, 6), BZH (46, 6), BZDH(46, 6),
2          BA (46, 6), BV (46, 6), BP(46, 6),
3          HTRR(46, 6), BTZZ(46, 6), BTKZ(46, 6),
4          ATTT(46, 6),
5          ASRR(46, 6), ASZZ(46, 6), ASRZ(46, 6),
6          HSTT(46, 6)
COMMON /CCM3/ TR (24,46), TRH (24,46), TRDH(24,46),
1          TZ (24,46), TZH (24,46), TZDH(24,46),
2          SR(46), SZ(46), TSR(46), TSZ(46), ZM(2,46), SPT4(5),
4          A1(2), A2(2), A3(2), A4(2), ALEN(2), AMAT(2), AMU(2), ANH(2),
5          BK(2), CAPE(2), CDOT(2), DR(2), DZ(2), RAD(2), PHO(2), RMT(2),
6          RHUG(2), RROT(2), TWMU(2), YTI(2), ZDOT(2), ZV(2), VCON(2),
7          CQ,DTN,DTM,DTMH,DTMIN,ZDINT,TYME,CHEKD,FACTR
COMMON /ICGM1/ IPTA(24,46)
COMMON /ICCM2/ IPTB(46, 6)
COMMON /ICCM3/ ISHP(2), JM(2), KM(2), KMID,
1  IRIIN, ICT1, IDT2, IDENT, IMAX, IPRNT, ICYCL, IMAP, NTT, KINT, KMN, KMX
   JJJ=JM(2)
   DO 350 J=1, JJJ
   AR(KMID,J)=BR(2,J)
   ARH(KMID,J)=BRH(2,J)
   ARDH(KMID,J)=BRDH(2,J)
   AZ(KMIC,J)=PZ(2,J)
   AZH(KMID,J)=BZH(2,J)
   AZDH(KMIC,J)=BZDH(2,J)
   ATRR(KMID,J)=BTPR(2,J)
   ATZZ(KMIC,J)=BTZZ(2,J)
   ATRZ(KMIC,J)=BTPZ(2,J)
   ATTT(KMID,J)=BTIT(2,J)
   ASRR(KMIC,J)=BSRR(2,J)
   ASZZ(KMIC,J)=BSZZ(2,J)
   ASRZ(KMID,J)=BSRZ(2,J)
   ASTT(KMIC,J)=BSTT(2,J)
   AA(KMID,J)=BA(2,J)
   AV(KMIC,J)=BV(2,J)
350 AP(KMIC,J)=BP(2,J)
C ****
C
C   FIND THE SWEEP BOUNCARIES
C
C ****
C   IF (ZDOT(1)) 300,301,300
300 KMN = 1
   JMX=JM(1)
   GO TO 303
301 IF (KMN-1) 303,303,303
302 KMN = KMN-1
303 IF (JMX-JM(1)) 304,305,305
304 JMX = JMX + 1
305 IF (KMX-KM(2)) 306,307,307
306 KMX = KMX + 1
C ****
C
C   CHECK IF THE TIME STEP HAS ATROPHIED BELOW THE ACCEPTABLE
C   LIMIT OF 10 PERCENT OF INITIAL TIME STEP
C

```

```

C ****
307 IF (DTH-OTMIN) 308,309,309
308 IMAX = ICYCL + 1
GO TO 310
C ****
C
C      N      N+1/2
C      FIND NEXT DELT AND DELT
C
C ****
309 OTN = (OT+DTH)/2.0
DTH = OT+DTH
CHEKD=OT+DTH
C ****
C
C      INCREMENT THE CYCLE COUNTER AND THE TIME VALUE
C
C ****
310 ICYCL = ICYCL + 1
TIME = TIME + DTH
RETURN
END
SUBROUTINE MMOV(I8,DELZ,DELZH, KLST,KEND,JM2)
IMPLICIT REAL*8 (A-H,O-Z,S), INTEGER (I-N)
COMMON /CCM1/ AR (24,46), ARH (24,46), ARDH(24,46),
1 A7 (24,46), AZH (24,46), AZDH(24,46),
2 AA (24,46), AV (24,46), AP (24,46),
3 ATRR(24,46), ATZZ(24,46), ATRZ(24,46),
4 ATTT(24,46),
5 ASRR(24,46), ASZZ(24,46), ASRZ(24,46),
6 ASTT(24,46)
COMMON /CCM2/ BR (46, 6), BRH (46, 6), BRDH(46, 6),
1 B7 (46, 6), BZH (46, 6), BZDH(46, 6),
2 BA (46, 6), BV (46, 6), BP(46, 6),
3 BTRR(46, 6), BTZZ(46, 6), BTRZ(46, 6),
4 BTTT(46, 6),
5 BSRR(46, 6), BSZZ(46, 6), BSRZ(46, 6),
6 BSTT(46, 6)
COMMON /CCM3/ TP (24,46), TRH (24,46), TRDH(24,46),
1 T7 (24,46), TZH (24,46), TZDH(24,46),
2 SP(46), SZ(46), TSR(46), TSZ(46), ZM(2,46), SPTM(5),
4 A1(2), A2(2), A3(2), A4(2), ALFN(2), AMAT(2), AMU(2), AMU(2),
5 BK(2), CAPE(2), CDCT(2), DR(2), DZ(2), RAD(2), RHD(2), RDC(2),
6 RHUG(2), RHLT(2), TWP(2), YT(2), ZOUT(2), ZV(2), VCUN(2),
7 CQ,DTN,DTF,OTHW,DTMIN,ZOINT,TIME,CHEKD,FACTR
COMMON /ICCM1/ IPTA(24,46)
COMMON /ICCM2/ IPTB(46, 6)
COMMON /ICCM3/ ISHP(2), JM(2), KM(2), KMID,
1 IRUN,IT1,IT2,IDENT,IMAX,IPRNT,ICYCL,IMAP,NTT,KINT,KMN,KFX
KSTRT=KLST+1
DO 300 K=KSTRT,KEND
DO 300 J=1,JM2
RZ(K,J)=BZ(K,J) + DELZ
300 RZH(K,J) = BZH(K,J) + DELZH
RETURN
END
SUBROUTINE FRAC (KK,SFS,IPT,KUX,R,Z,RH,ZH,RDH,ZDH,TRR,TZ7,TRZ,TTT,
1 SRQ,SZZ,SRZ,STT,P,JLST)
IMPLICIT REAL*8 (A-H,O-Z,S), INTEGER (I-N)
DIMENSION IPT(KUX,1),

```

```

1  R(KUX,1), Z(KUX,1), RH(KUX,1), ZH(KUX,1), RDH(KUX,1),
2  ZDH(KUX,1), TRR(KUX,1), TZZ(KUX,1), TRZ(KUX,1), TTT(KUX,1),
3  SRK(KUX,1), SZZ(KUX,1), SRZ(KUX,1), STT(KUX,1), P(KUX,1)
COMMON /CCM3/ TR (24,46), TRH (24,46), TRDH(24,46),
1  T7 (24,46), TZH (24,46), TZDH(24,46),
2  SR(46), SZ(46), TSR(46), TSZ(46), ZH(2,46), SPTH(5),
4  A1(2), A2(2), A3(2), A4(2), ALEN(2), AMAT(2), AMH(2), ANH(2),
5  BK(2), CAPE(2), CDOT(2), DR(2), DZ(2), RAD(2), RHO(2), RDOT(2),
6  RHUG(2), RHLT(2), TWP(2), YT(2), ZDOT(2), ZV(2), VCON(2),
7  CQ,DTN,CTF,DTHW,DTMIN,ZDINT,TYME,CHEKO,FACTR
COMMON /ICCM3/ ISHP(2), JM(2), KM(2), KMID,
1  IKUN,ICY1,IDT2,IDENT,IMAX,IPRNT,ICYCL,IMAP,NTT,KINT,KMN,KMX
NPR=6
KCOL=KK
IF (KCOL.EC.1) RETURN
DO 302 J=2,JLST
SHR=TRZ(KK,J)
IF (DABS(SHR)-SHS) 302,300,300
300 IP = IPT(KK,J)
JM1=J-1
JP1=J+1
IPL=IPT(KK,JM1)
IF (((IP.GT.13).AND.(IP.LT.20)).OR.((IPL.GT.13).AND.(IPL.LT.20)))
1 GO TO 302
WRITE (NPR,100) KK,J
100 FORMAT (1H0, '**** SHEAR FRACTURE **** AT K=',I5,'X',I5,I5/)
TR (KCOL,J) = R (KK,J)
TZ (KCOL,J) = Z (KK,J)
TRH (KCOL,J) = RH (KK,J)
TZH (KCOL,J) = ZH (KK,J)
TRDH(KCOL,J) = RDH(KK,J)
TZDH(KCOL,J) = ZDH(KK,J)
IF (IP.EC.5) GO TO 9
IF (IP.EC.1) GO TO 1
IF (IP.EC.7) GO TO 7
GO TO 302
7 IPT(KK,J) = 14
IPT(KK,JP1)=21
GO TO 330
1 IPT(KK,J)=15
IPT(KK,JP1)=22
GO TO 330
7 IPT(KK,J)=16
IPT(KK,JP1)=23
330 CONTINUE
DO 300C II=1,2
JJ=J+II-1
KM1=KK-1
KM1N1=KM1
JM1=JJ-1
TRRW=TRR(KK,JJ)
TZZW=TZZ(KK,JJ)
TRZW=TRZ(KK,JJ)
TTTW=TTT(KK,JJ)
IP=IPT(KK,JJ)
R1=TR(KK,JJ)
Z1=TZ(KK,JJ)
IPLFF=IPT(KK-1,JJ)
IF (((IPLFF.GT.13).AND.(IPLFF.LT.20)) GO TO 5101
GO TO 5102

```

```

5101 Z2=TZ(KK-1,JJ)
    R2=TR(KK-1,JJ)
    GO TO 5103
5102 Z2=Z(KK-1,JJ)
    R2=R(KK-1,JJ)
5103 CONTINUE
    IPR=IPT(KM1,JM1)
    IF ((IPR.GT.13).AND.(IPR.LT.20)) GO TO 5019
    GO TO 5018
5019 Z3 = TZ(KMIN1,JM1)
    R3 = TR(KMIN1,JM1)
    GO TO 5020
5019 Z3=Z(KM1,JM1)
    R3=R(KM1,JM1)
5020 IPR=IPT(KK,JM1)
    IF ((IPR.GT.13).AND.(IPR.LT.20)) GO TO 5021
    GO TO 5022
5021 Z4=TZ(KK,JJ-1)
    R4=TR(KK,JJ-1)
    GO TO 5023
5022 Z4=Z(KK,JM1)
    R4=R(KK,JM1)
5023 CONTINUE
    CALL FRFESL (I,R1,Z1,R2,Z2,R3,Z3,R4,Z4,TRRW,TZZW,TRZW,TTTW,SRPW,
    1SZZW,SPZW,STTW,KK,IP,PW)
    TRR(KK,JJ)=TRRW
    TZZ(KK,JJ)=TZZW
    TRZ(KK,JJ)=TRZW
    TTT(KK,JJ)=TTTW
    P(KK,JJ)=PW
    SRR(KK,JJ)=SRRW
    SZZ(KK,JJ)=SZZW
    SRZ(KK,JJ)=SPZW
    STT(KK,JJ)=STTW
3000 CONTINUE
302 CONTINUE
    RETURN
    END
SUBROUTINE FRACTN (TRP,TZZ,TRZ,TTT,K,KUX,R,Z,RH,ZH,RDH,ZDH,J1,
1ISTR,SRR,SZZ,SRZ,STT,P,IPT)
    IMPLICIT REAL*8 (A-H,O-Z,S), INTEGER (I-N)
    DIMENSION IPT(KUX,1),
    1 R(KUX,1), Z(KUX,1), RH(KUX,1), ZH(KUX,1), RDH(KUX,1),
    2 ZDH(KUX,1), TRR(KUX,1), TZZ(KUX,1), TRZ(KUX,1), TTT(KUX,1),
    3 SRR(KUX,1), SZZ(KUX,1), SRZ(KUX,1), STT(KUX,1), P(KUX,1)
    COMMON /CCM3/ TR (24,46), TRH (24,46), TRDH(24,46),
    1 TZ (24,46), TZH (24,46), TZDH(24,46),
    2 SR(46), SZ(46), TSR(46), TSZ(46), ZM(2,46), SPTM(5),
    4 A1(2), A2(2), A3(2), A4(2), ALFN(2), AMAT(2), AMU(2), AMU(2),
    5 BK(2), CAPF(2), CDDT(2), DR(2), DZ(2), PAD(2), RHU(2), RDOT(2),
    6 RHUG(2), RDOT(2), TWMI(2), YI(2), ZDOT(2), ZV(2), VCON(2),
    7 CQ,DTN,CTH,CTH,DTMIN,ZDINT,TYME,CHEKD,FACTR
    NPR=6
    KP1=K+1
    DO 370 J=2,J1
    STR=TRP(K,J)
    STZ=TZZ(K,J)
    STRZ=TRZ(K,J)
    FCUN=0.5*(STR+STZ)
    TCUN=0.5*(STZ-STR)

```

```

      IF (DABS(TCON)) 430,430,429
429  SBC=STRZ/TCCN
      PHI=DATAN(SBC)
      GO TO 431
430  PHI=0.0
431  ALPHA=DSIN(PHI)
      BETA=DCOS(PHI)
      TZZP=ECCA+TCON*BETA +STRZ*ALPHA
      TRRP=-TZZP+STZ+STR
      PHI=90.0*PHI/3.1415928
      IF (TZZP-TRRP) 302,303,303
302  IF (TRRP) 312,312,314
314  TNS=TRRP
      GO TO 322
303  IF (TZZP) 312,312,324
324  TNS=TZZP
      GO TO 322
322  IF (TNS-STR) 312,326,326
326  JM1=-1
328  WRITE (APR,100) K,J,PHI
100  FORMAT(1H0,'****SPALL****AT K=',I5,5X,'J=',I5,'ANGLE='FR.2)
      IPT(K,J)=10
      TRR(K,J)=C.0
      TZZ(K,J)=0.0
      TRZ(K,J)=0.0
      PW=-TTT(K,J)/3.0
      P(K,J)=PW
      SRR(K,J)=PW
      STT(K,J)=-2.0*PW
      SRZ(K,J)=0.0
      SZT(K,J)=PW
      TRR(KP1,J)=0.0
      TZZ(KP1,J)=0.0
      TRZ(KP1,J)=0.0
      PW=-TTT(K,J)/3.0
      P(KP1,J)=PW
      SRR(KP1,J)=PW
      SZT(KP1,J)=PW
      SRZ(KP1,J)=0.0
      STT(KP1,J)=-2.0*PW

      ZI=Z(K,JP1)
      RI=R(KP1,J)
      ZA=Z(K-1,JP1)
      RA=R(K-1,JP1)
      ZB=Z(K-1,J)
      RB=R(K-1,J)

      ZC=Z(K,J)
      RC=R(K,J)
      IP=22
      TRRW=TRR(K,JP1)
      TZZW=TZZ(K,JP1)
      TRZW=TRZ(K,JP1)
      TTTW=TTT(K,JP1)
      CALL FREESU (1,RI,ZI,RA,ZA,RR,ZB,RC,ZC,TRRW,TZZW,TRZW,TTTW,
1SRRW,SZZW,SRZW,STTW,K,IP,PW)
      TRR(K,JP1)=TRRW
      TZZ(K,JP1)=TZZW
      TRZ(K,JP1)=TRZW

```

```

      TTT(K,JP1)=TTTW
      P(K,JP1)=PW
      SRR(K,JP1)=SRRW
      SZZ(K,JP1)=SZZW
      SRZ(K,JP1)=SRZW
      STT(K,JP1)=STTW
      IPT(K,JM1)=1R
      JP1=J+1
      IPT(K,JP1)=22
      IP1=IPT(KP1,J)
      IF (IP1.FQ.22) IPT(KP1,J)=20
      TR(K,J)=20
      TZ(K,J)=Z(K,J)
      TRH(K,J)=RH(K,J)
      TZH(K,J)=ZH(K,J)
      TRDH(K,J)=RDH(K,J)
      TZDH(K,J)=ZDH(K,J)
      TR(K,JM1)=R(K,JM1)
      TZ(K,JM1)=Z(K,JM1)
      TRH(K,JM1)=RH(K,JM1)
      TZH(K,JM1)=ZH(K,JM1)
      TRDH(K,JM1)=RDH(K,JM1)
      TZDH(K,JM1)=ZDH(K,JM1)
312 CONTINUE
3000 CONTINUE
      RETURN
      END
      SUBROUTINE GUTT (IR ,IPT,R,Z,RH,ZH,RDH,ZDH,TRR,TZZ,TRZ,TTT,SRR,
1          SZZ,SRZ,STT,A,V,P,KUX,KMIN,KMAX,JMAX)
      IMPLICIT REAL*8 (A-H,O-Z,S), INTEGER (I-N)
      COMMON /CCM3/ TR (24,46), TRH (24,46), TRDH(24,46),
1          T7 (24,46), TZH (24,46), TZDH(24,46),
2          SR(46), SZ(46), TSR(46), TSZ(46), ZM(2,46), SPTM(5),
4          A1(2), A2(2), A3(2), A4(2), ALEN(2), AMAT(2), AMU(2), ANU(2),
5          BK(2), CAPE(2), CDDT(2), DR(2), DZ(2), RAD(2), RHO(2), RDOT(2),
6          RHOG(2), RHOT(2), TWMU(2), YT(2), ZDOT(2), ZV(2), VCUN(2),
7          CQ,DTN,DTF,DTHW,DTMIN,ZDINT,TYMF,CHEKD,FACTR
      COMMON /ICLM3/ ISHP(2), JM(2), KM(2), KMID,
1          IRUN,INT1,INT2,IDENT,IMAX,IPRNT,ICYCL,IMAP,INT,KINT,KMN,KMX
      DIMENSION
1          IPT(KUX,1),
1          R(KUX,1), RH(KUX,1), RDH(KUX,1),
2          Z(KUX,1), ZH(KUX,1), ZDH(KUX,1),
3          TRR(KUX,1), TZZ(KUX,1), TRZ(KUX,1), TTT(KUX,1),
4          SRR(KUX,1), SZZ(KUX,1), SRZ(KUX,1), STT(KUX,1),
5          A(KUX,1), V(KUX,1), P(KUX,1)
      NPR=6
      SHS =A1(IR)
C *****
C
C      INITIALISE TO ZERO VARIOUS VARIABLES
C
C *****
      TRRA =0.0
      TRRB =0.0
      TRRC=0.0
      TRRD=0.0
      TZZA=0.0
      TZZB=0.0
      TZZC=0.0

```



```

T7ZD=0.0
TRZA=0.0
TRZH=0.0
TRZC=0.0
TRZD=0.0
ACUNA=0.0
ACUNB=0.0
ACUNC=0.0
ACUND=0.0
BCUNA=0.0
BCUNB=0.0
BCUNC=0.0
BCUND=0.0
PCUNA=0.0
PCUNB=0.0
PCUNC=0.0
PCUND=0.0
Z12=0.0
Z23=0.0
Z34=0.0
Z41=0.0
P12=0.0
R23=0.0
R34=0.0
R41=0.0
DO 3001 K= KMIN, KMAX
  KMIN1 = K-1
  KPLS1 = K+1
  KMI = KMIN1
  KCUR= K
  KP1 = KPLS1
401 DO 3000 J=1, JMAX
  JM1 = J-1
  JP1 = J+1
  IP = IPT(K,J)
  IF (K.CT.1) IPLFF=IPT(KMIN1,J)
501 ITA=0
  ITB=0
  ITC=0
  ITD=0
  ITS=0
  IT1A=0
  IT1B=0
  IT1C=0
  IT1D=0
5002 GO TO (5001,5001,5001,5001,5001,5001,5004,5004,5001,5001,5001,
1      5001,5001,5001,5001,5004,5004,5001,5004,5001,5004,5001,
2      5004,5004,5002,5004,5004,5002,5002),IP
5001 R1 = R(KP1,J)
  Z1 = Z(KP1,J)
  GO TO 5004
5002 IPR=IPT(KP1,J)
  IF ((IPR.GT.13).AND.(IPR.LT.26)) GO TO 5003
  GO TO 5001
5003 R1 = TR(KPLS1,J)
  Z1 = T7(KPLS1,J)
5004 CONTINUE
5005 GO TO (5005,5005,5005,5005,5005,5005,5006,5005,5006,5005,5006,5005,
1      5005,5005,5006,5006,5006,5006,5006,5005,5006,5005,5005,
2      5005,5005,5005,5005,5006,5226,5226),IP
5005 R2 = R(KCUR,JP1)

```

```

      Z2 = Z(KCUR,JP1)
5226 IPR=IPT(K,JP1)
      IF ((IPR.GT.13).AND.(IPR.LT.20)) GO TO 5227
      GO TO 5005
5227 R2=TR(K,JP1)
      Z2=TZ(K,JP1)
5006 CONTINUE
      GO TO (5007,5007,5010,5007,5010,5010,5007,5007,5007,5007,5007,
1      5007,5007,5007,5007,5007,5010,5007,5007,5009,5007,5007,5007,
2      5008,5008,5008,5010,5010,5008),IP
5007 R3=R(KM1,J)
      Z3=Z(KM1,J)
      GO TO (5036,5034),IR
5036 IF ((K.EQ.KMIN).AND.(K.GT.1)) GO TO 5035
5034 CONTINUE
      GO TO 5010
5035 SR(J)=R3
      SZ(J)=73
      GO TO 5010
5009 R3=TR(KM1,J)
      Z3=TZ(KM1,J)
      GO TO 5010
5008 IPR=IPT(KM1,J)
      IF ((IPR.GT.13).AND.(IPR.LT.20)) GO TO 5009
5010 R3=RTMP
      Z3=ZTMP
5010 CONTINUE
      GO TO (5011,5014,5014,5014,5011,5011,5011,5011,5011,5011,5011,
1      5011,5014,5011,5011,5011,5014,5011,5012,5013,5013,5013,
2      5013,5014,5014,5014,5014,5014,5013),IP
5011 IPR=IPT(K,JM1)
      IF ((IPR.GT.13).AND.(IPR.LT.20)) GO TO 5013
5012 R4 = R(KCUR,JM1)
      Z4 = Z(KCUR,JM1)
      GO TO 5014
5013 R4 = TR(K,JM1)
      Z4 = TZ(K,JM1)
5014 CONTINUE
      GO TO (4000,4001),IR
4000 IF (K=1) 4003,4003,4001
4001 IF (K=KMIN) 4002,4002,4003
4002 SR(J)=R(KM1,J)
      SZ(J)=7(KM1,J)
4003 CONTINUE
305 GO TO (1,2,3,4,5,6,7,8,9,10,11,12,13,14,15,16,17,18,19,20,21,22,
1      23,24,25,26,27,28,29),JP
1 ITA=1
  ITB=1
  ITC=1
  ITD=1
  GO TO 704
2 ITS=1
  ITA=1
  ITB=1
  GO TO 702
3 ITS=1
  ITA=1
  GO TO 701
4 ITS=1
  ITB=1

```

NOT REPRODUCIBLE

```

      ITDA=1
      GO TO 702
5  ITA=1
   ITD=1
   ITUC=1
   GO TO 704
6  ITD=1
   ITUC=2
   GO TO 704
7  ITB=1
   ITC=1
   ITDA=1
   GO TO 703
8  ITC=1
   ITDB=1
   GO TO 703
9  ITB=1
   ITC=1
   ITD=1
   ITDA=1
   GO TO 704
10 ITC=1
   ITD=1
   ITDA=1
   GO TO 704
11 CONTINUE
   GO TO 1
12 CONTINUE
   GO TO 1
13 ITA=1
   ITB=1
   ITS=1
   GO TO 702
14 CONTINUE
   GO TO 10
15 CONTINUE
   GO TO 10
16 CONTINUE
   GO TO 8
17 CONTINUE
   GO TO 3000
18 CONTINUE
   GO TO 9
19 CONTINUE
   GO TO 8
20 CONTINUE
   GO TO 1
21 CONTINUE
   GO TO 7
22 CONTINUE
   GO TO 1
23 CONTINUE
   GO TO 7
24 CONTINUE
   ITB=1
   ITDA=1
   GO TO 702
25 ITA=1
   ITB=1
   GO TO 702

```

```

26 CONTINUE
  GO TO 24
27 CONTINUE
  GO TO 3000
28 ITA=1
  GO TO 701
29 ITA=1
  ITR=1
  ITD=1
  ITUC=3
704 Z41 = Z4-Z1
  R41 = R4-F1
  TRRD = TRRA
  TZZD = TZZA
  TRZD = TRZA
  PCUND= PCCNA
  ACUND= ACCNA
  BCUND= HCCNA
  IF (ITCC-EQ.3) GO TO 702
  IF (ITOC-2) 306,313,306
306 IF (ITCC-1) 703,701,703
703 Z34=Z3-Z4
  R34=R3-R4
  TRRC = TRRB
  TZZC = TZZB
  TRZC = TRZB
  PCUNC= PCCNB
  ACUNC= ACCNB
  BCUNC= HCCNB
  IF (ITCB-1) 307,313,307
307 IF (ITCB-2) 702,701,702
702 Z23 = Z2-Z3
  R23 = R2-R3
  TRR3 = TRR(KCUR,JP1)
  TZZ3 = TZZ(KCUR,JP1)
  TRZ3 = TRZ(KCUR,JP1)
  AN = A (KCUR,JP1)
  AMASS = AN/ZM(IR,JP1)
  PCUNB = RHL(IR)*AN/ V(KCUR,JP1)
  ACUNB = TRZB*AMASS
  BCUNB = (TRRH - TTT(KCUR,JP1))*AMASS
308 IF (ITCA-1) 701,313,701
701 Z12= Z1-Z2
  R12= R1-F2
  TRRA= TRR(KP1,JP1)
  TZZA= TZZ(KP1,JP1)
  TRZA= TRZ(KP1,JP1)
  AN = A (KP1,JP1)
  GO TO (309,311),IR
309 IF (K-KINT) 311,310,311
310 AMASS = AN/ZM(2,JP1)
  PCUNA = RHC(2)*AN/ V(KP1,JP1)
  GO TO 312
311 AMASS = AN/ZM(IR,JP1)
  PCUNA = RHC(IR)*AN/V(KP1,JP1)
312 ACUNA = TRZA*AMASS
  BCUNA = (TRRA-TTT(KP1,JP1))*AMASS
313 IF (IP.GT.23) GO TO 5016
C ****
C

```

C EQUATIONS OF MOTION

C

C ****

```

5015 ZN=Z(KCUR,J)
      RN=R(KCLR,J)
      RDHF=RDH(KCUR,J)
      ZDHF=ZDH(KCUR,J)
      GU TO 5017
5016 ZN=TZ(K,J)
      RN=TR(K,J)
      RDHF=TRDH(K,J)
      ZDHF=TZCH(K,J)
5017 CONTINUE
      PHI=(ITA*PCONA + ITB*PCONB + ITC*PCONC + ITD*PCOND)*1.0017/4.0
      RZDCN = ITA/(2*PHI)
      IF (ITS-1) 315,314,315
314 RNW=0.0
      RNH=0.0
      RDNH=0.0
      ALFA=0.0
      GU TO 318
315 TCNH= 1.0/(ITA+ITB+ITC+ITD)
      ALFA= TCNH*(ITA*ACONA + ITB*ACONB + ITC*ACONC + ITD*ACOND)
      BETA= TCNH*(ITA*BCONA + ITB*BCONB + ITC*BCONC + ITD*BCOND)
      RDNH= RDHF + RZDCN*(ITA*(TRRA*Z12-TR7A*R12) + ITB*(TRRB*Z23
1      -TRZB*R23) + ITC*(TRRC*Z34-TRZC*R34) + ITD*(TRRD*Z41-TRZD*
2      R41)) + ITN*BETA
      RDEF = RDNH*CTH
      RNW = RN+RDEF
      IF (DABS(RDEF)-1.00-07) 316,316,317
316 RNW = RN
317 RNH = (RNH+RN)/2.0
318 ZDWH= ZDHF -RZDCN*(ITA*(TZZA*R12-TRZA*Z12) + ITB*(TZZB*R23
1      -TRZB*Z23) + ITC*(TZZC*R34-TRZC*Z34) + ITD*(TZZD*R41-TRZD*
2      Z41)) + CTN*ALFA
      ZDEF =ZCAH*CTH
      ZNW = ZN+ZDEF
      IF (DABS(ZDEF)-1.00-07) 319,319,320
319 ZNW = ZN
320 ZNH = (ZN +ZNW)/2.0
      IF (ITC) 322,321,322
321 PHI=0.0
      GU TO 339

```

C ****

C

C

C

C

C ****

```

322 Z1= ZNW
      R1= RNW
      IF ((IPLEF.GT.1).AND.(IPLEF.LT.20)) GU TO 5101
      GU TO 5102
5101 Z2=TSZ(J)
      R2=TSR(J)
      RH2=TRH(KM1,J)
      ZH2=TZH(KM1,J)
      RDH2=TRDH(KM1,J)
      ZDH2=TZCH(KM1,J)
      GU TO 5103
5102 Z2=SZ(J)

```

NOT REPRODUCIBLE

```

R2=SR(J)
RH2=RH(KM1,J)
ZH2=ZH(KM1,J)
RDH2=RDH(KM1,J)
ZDH2=ZDH(KM1,J)
5102 CONTINUE
IPR=IPT(KM1,JM1)
IF ((IPR.GT.13).AND.(IPR.LT.20)) GO TO 5019
GO TO 5018
5019 Z3 = TZ(KMIN1,JM1)
R3 = TR(KMIN1,JM1)
ZH13 = ZAH-TZH(KMIN1,JM1)
RH13 = RAH-TRH(KMIN1,JM1)
ZDH13 = ZDAH-TZDH(KMIN1,JM1)
RDH13 = RDAH-TRDH(KMIN1,JM1)
GO TO 5020
5018 Z3=Z(KM1,JM1)
R3=R(KM1,JM1)
ZH13 = ZNH - ZH(KM1,JM1)
RH13 = PAH - PH(KM1,JM1)
ZDH13=ZDAH - ZDH(KM1,JM1)
RDH13=RDAH - RDH(KM1,JM1)
5020 IPR=IPT(K,JM1)
IF ((IPR.GT.13).AND.(IPR.LT.20)) GO TO 5021
GO TO 5022
5021 Z4=TSZ(JM1)
R4=TSR(JM1)
ZH42 = TZH(K,JM1) - ZH2
RH42 = TRH(K,JM1) - RH2
RDH42 = TRDH(K,JM1) - RDH2
ZDH42 = TZDH(K,JM1) - ZDH2
GO TO 5023
5022 Z4 = SZ(JM1)
R4 = SR(JM1)
RH42 = RH(KCUR,JM1)-RH2
ZH42 = ZH(KCUR,JM1)-ZH2
ZDH42=ZDH(KCUR,JM1) - ZDH2
RDH42=RDH(KCUR,JM1) - RDH2
5023 CONTINUE
C ****
C
C   COMPUTE THE AREA AND RELATIVE VOLUME AT NEW TIME
C
C ****
AN= A(KCUR,J)
VN= V(KCUR,J)
Z42=Z4-Z2
R42=R4-R2
A124=0.5*(Z4*(R1-R2)-Z1*R42+Z2*(R4-R1))
A234=0.5*(Z4*(R2-R3)+Z2*(R3-R4)+Z3*R42)
AW=A124+A234
AH=0.5*(AW+AN)
VW=RHUT(IPR) * (A124*(R4+R1+R2)+A234*(R3+R4+R2))/Z4(IH,J)
VH=0.5*(VW+VN)
DELVV=(VW-VN)/VH
IF (JABS(DELVV)-1.0E-07) 323,323,324
323 DELVV=0.0
C ****
C
C   COMPUTE THE STRAIN INCREMENTS

```

NOT REPRODUCIBLE

```

C
C ****
324 ECCN = 0.5*QTH/AH
EZZH = ECCN * (ZDH42*RH13 - RH42*ZDH13)
ERRH = -ECCN * (RDH42*ZH13 - ZH42*RDH13)
ERZH = ECCN * (RDH42*RH13 - RH42*RDH13 - ZDH42*ZH13 + ZDH13*ZH42)
ETTH = DELVV - EZZH - ERRH
SCUNC = DELVV/3.0
SZZN = SZZ(KCUR,J)
SRRN = SRR(KCUR,J)
SRZN = SRZ(KCUR,J)
ALFA = 0.5*ECCN*(RDH42*RH13 - RH42*RDH13 + ZDH42*ZH13 - ZH42*ZDH13)
BETA = 2.0*5*ZNA*ALFA
C ****
C
C COMPUTE NEW STRESS DEVIATORS
C
C ****
SZZW = SZZN + TWMU(1R)*(EZZH-SCUNC)+BETA
SRRW = SRRN + TWMU(1R)*(ERRH-SCUNC)-BETA
SRZW = SRZN + AMU(1D)*ERZH + (SRRN-SZZN)*ALFA
STTW = STT(KCUR,J) + TWMU(1B)*(ETTH-SCUNC)
C ****
C
C COMPUTE THE ARTIFICIAL VISCOSITY TERMS
C
C ****
IF (DELVV) 326,325,325
325 QCNH = 0.0
GO TO 327
326 VDJV = DELVV/QTH
QCNH = (AH*PH*(1B)/VH)*(CQ*VDJV)**2
C ****
C
C USE THE EQUATION OF STATE TO COMPUTE THE PRESSURE INCREMENT
C
C ****
327 DELP = -PK(1B)*DELVV
PW = P(KCUR,J)+DELP
C ****
C TOTAL STRESSES ARE COMPUTED NEXT
C ****
TZZW = SZZW-PW-QCNH
TPRW = SRRW-PW-QCNH
TRZW = SRZW
TTTW = STTW-PW-QCNH
C ****
C
C CALL THE FREE SURFACE ROUTINE TO ADJUST THE STRESS VALUES
C
C ****
CALL FREESU(14,R1,Z1,R2,Z2,R3,Z3,R4,Z4,TPRW,TZZW,TRZW,TTTW,
1 SRKW,SZZW,SRZW,STTW,K,IP,PW)
C ****
C
C COMPUTE THE PRINCIPAL STRESSES
C
C ****
328 ECUN = 0.5*(TZZW+TPRW)
TCCN = 0.5*(TZZW-TPRW)

```

```

      IF (DABS(TCCN)) 320,330,329
329 PHI=DATAA(TRZW/TCCN)
      GO TO 331
330 PHI=0.0
331 ALFA =DSIN(PHI)
      BETA =DCCS(PHI)
      TZZP = ECCN + TCON*BETA +TRZW*ALFA
      TRRP = -TZZP +TZZh + TRRW
      PHI =90.0*PHI/3.1415928
C ****
C
C   CHECK FOR TIME STEP STABILITY
C
C ****
332 RR13= (R1-R3)**2 + (I1-I3)**2
      RR24= R42*R42 + Z42*Z42
      IF (RR13 - RR24) 333,333,334
333 DELR =DSCRT(RR13)
      GO TO 335
334 DELR =DSCRT(RR24)
335 CHECKO=(DELR/CDCT(I1))*FACTP
336 CONTINUE
      GO TO (336,339),IH
336 IF (K-KMIN)337,337,339
337 IF (J-1)338,338,339
338 KT=K
      JT=J
      DTHW=CHECKO
339 IF (CHECKO-DTHW) 340,340,341
340 KT=K
      JT=J
      DTHW = CHECKO
341 IF (4J0(ICYCL,IPRNT)) 351,342,351
342 IF (J-1) 350,343,350
343 IF (IR-1) 346,344,346
344 IF (K-KMIN) 347,345,349
C ****
C
C   FIND THE WAVE FRONT POSITION
C
C ****
345 WF = TIME*CDCT(I)
      KWF =IDINT(WF/0.2(1)+0.5)
      WRITE (NPR,100) ICYCL,TIME,WF,KWF,DTH,DTHW,IJT,KT,JT
346 IF (IH-2) 349,347,349
347 IF (K-2) 349,348,349
348 WRITE (NPR,101) KINT
349 WRITE (NPR,102) IR,K
      TZZP = 0.0
      TRRP = 0.0
      PHI = 0.0
      TZZh = 0.0
      TRRW = 0.0
      TRZW = 0.0
      TITW = 0.0
C ****
C
C   WRITE OUT THE RESULTS
C

```

NOT REPRODUCIBLE


```

C ****
350 WRITE (NPR,103) J,ZNW,RNW,TZZW,TRRW,TRZW,TTTW,TZZP,TRRP,PHI
C ****
C
C     TRANSFER DATA (GEOMETRIC) OF K-1 POINTS FROM TEMPORARY STORAGE
C     TO PERMANENT STORAGE
C
C ****
351 IF (K-1) 353,353,352
352 IF ((IP.GT.23) GO TO 6001
    IF ((IP.GT.13).AND.(IP.LT.27)) GO TO 6002
    R(KM1,J)=SR(J)
    Z(KM1,J)=SZ(J)
    SR(J)=RNW
    SZ(J)=ZNW
    IF ((IPLEF.GT.13).AND.(IPLEF.LT.27)) GO TO 6003
    GO TO 6009
6001 IF ((IPLEF.GT.13).AND.(IPLEF.LT.27)) GO TO 6004
    GO TO 6005
6004 TR(KM1,J)=TSR(J)
    TZ(KM1,J)=TSZ(J)
6005 TSR(J)=RNW
    TSZ(J)=ZNW
    GO TO 6009
6002 IF ((IPLEF.GT.13).AND.(IPLEF.LT.27)) GO TO 6007
6007 RTEMP=R(KM1,J)
    ZTEMP=Z(KM1,J)
6007 R(KM1,J)=SR(J)
    Z(KM1,J)=SZ(J)
    353 SR(J)=RNW
    SZ(J)=ZNW
    GO TO 6009
6003 TR(KM1,J)=TSR(J)
    TZ(KM1,J)=TSZ(J)
6009 CONTINUE
    IF (IP.GT.23) GO TO 5026
    RH(KCUR,J)=RNH
    ZH(KCUR,J)=ZNH
    RDH(KCUR,J)=RDNH
    ZDH(KCUR,J)=ZDNH
    GO TO 5027
5026 TRH(K,J)=RNH
    TZH(K,J)=ZNH
    TRDH(K,J) = PDNH
    TZDH(K,J) = ZDNH
5027 CONTINUE
    IF (ITC-1)3000,354,3000
354 A(KCUR,J)=AW
    V(KCUR,J)=VW
    P(KCUR,J)=PW
    SZZ(KCLF,J)=SZZW
    SRR(KCUR,J)=SRPW
    SRZ(KCUR,J)=SRZW
    STT(KCUR,J)=STTW
    TZZ(KCUR,J)=TZZW
    TRR(KCUR,J)=TRRW
    TRZ(KCUR,J)=TRZW
    TTT(KCUR,J)=TTTW
    IF (IP.GT.23) GO TO 300
    IF ((IP.GT.13).AND.(IP.LT.27)) GO TO 5030

```

NOT REPRODUCIBLE

NOT REPRODUCIBLE

```

      SZZW=PW
      GU TO 1
7     Z1=Z0
      R1=R0
      Z2=ZC
      R2=RC
      GU TO 300
10    IF ((K.EQ.2).AND.(IR.EQ.1)) GO TO 9
      Z1=Z0
      R1=R0
      R2=RA
      Z2=ZA
      R2=RA
      GO TO 300
12    Z1=ZA
      R1=RA
      Z2=ZB
      R2=RA
      GO TO 300
22    Z1=ZB
      R1=RB
      Z2=ZC
      R2=RC
      GO TO 300
300   Q1=R1-R2
      IF (DABS(Q1)-1.00-05) 301,301,302
301   ETA=0.0
      GU TO 310
302   D2=Z1-Z2
      IF (DABS(D2)-1.00-05) 303,303,304

303   ETA=PI/2.0
      GO TO 310
304   ETA=ATAN((R1-R2)/(Z1-Z2))
310   ALPHA=2.0*ETA
      TSTW=((TRRW+TZZW)/2.0)+0.5*(TZZW-TRRW)*DCOS(ALPHA)+TRZW*
      SINS(ALPHA)
      TRRW=0.5*TSTW*(1.0-DCOS(ALPHA))
      TZZW=0.5*TSTW*(1.0+DCOS(ALPHA))
      TRZW=0.5*TSTW*SINS(ALPHA)
      PW=-(TRRW+TZZW+TTTW)/3.0
      SRRW=TRRW+PW
      SZZW=TZZW+PW
      SRTW=TRZW
      STTW=TTTW+PW
1     CONTINUE
      RETURN
      END
//GO,SYSIN DD, *
      1
      6001      0711      70      0.5
      2          1          31          1
      1000
      100      0.29 273000.0      0.92      140.0
70.0
      2          0.0          0.0          45          22          0.125          0.125
      ALM  0.29 1000000.0      2.7 150000.0
75000.0
      1          0.0          -7.7          5          45          0.125          0.125
/*

```

NOT REPRODUCIBLE

REFERENCES

1. Ross, Bernard, Penetration Studies of Ice with Application to Arctic and Subarctic Warfare; for Submarine Arctic Warfare and Scientific Program, Contract Nonr-2332(00), Stanford Research Institute, Menlo Park, Calif., November 1965
2. Ross, Bernard, Penetration Studies of Ice with Application to Arctic and Subarctic Warfare - Phase II Study; for Submarine Arctic Warfare and Scientific Program, Contract Nonr-2332(00), Stanford Research Institute, Menlo Park, Calif., May 1967
3. Ross, Bernard and S. Hanagud, Penetration Studies of Ice with Application to Arctic and Subarctic Warfare, Final Report; for Submarine Arctic Warfare and Scientific Program, Contract N00014-68-A-0243, Stanford Research Institute, Menlo Park, Calif., September 1969
4. Hanagud, S., B. Ross, and G. Sidhu, "Elastic-Plastic Impact of Plates," Israel Journal of Technology, Vol. 7, No. 1-2, 1969 and Proceedings of the Eleventh Annual Conference on Aviation and Astronautics, Haifa, Israel, 5-6 March 1969, pp. 149-161
5. Hanagud, S., B. Ross, and G. Sidhu, "Elastic-Plastic Impact of Rods and Plates in Compactible Materials," submitted for publication to J. Appl. Mech., Amer. Soc. Mech. Engr.
6. Sidhu, G., S. Hanagud, and B. Ross, "Proper Treatment of Boundary Conditions for Two-Dimensional Shock Wave Propagation Computer Codes," to be submitted for publication to J. Appl. Phys.
7. Hanagud, S., B. Ross, and G. Sidhu, Large Deformation, Elastic-Plastic Analysis of Ice-Structure Interaction, presented at IAHR Ice Symposium, Reykjavik, Iceland, August 1970, to be published in J. of Hydraulic Research, Delft, Holland
8. Sidhu, G., B. Ross, and S. Hanagud, Plane Stress Problems of Arctic Sea Ice--Hydraulic Structure Interaction, to be presented at First International Conference on Port and Ocean Engineering Under Arctic Conditions, Trondheim, Norway, August 1971
9. Ross, Bernard, "Penetration and Fracture of Sea Ice Due to Impact Loading," Proc. of the International Conference on the Physics of Ice and Snow, ed. by Z. Yosida, Hokkaido University, Sapporo, Japan, August 1966, pp. 499-522

10. Ross, Bernard, "The Perforation of a Porous Medium Due to Projectile Impact," *Experimental Mechanics*, Vol. 8, No. 11, November 1968, pp. 488-495
11. Hanagud, S., and B. Ross, "Large Deformation Deep Penetration Theory for a Compressible, Strain-Hardening Target Material," presented at the AIAA Hypervelocity Impact Conference, Cincinnati, Ohio, April 30-May 2, 1969, accepted for publication in the AIAA Journal
12. Ross, Bernard, "Perforation of the Arctic Sea Ice Cover by Projectile Impact," *J. Hydronautics*, Vol. 3, No. 3, July 1969, pp. 115-120
13. Hanagud, S., "Snow as a Locking Material--High Pressure Properties of Snow," *Proc. of the International Conference on the Physics of Ice and Snow*, Vol. 2, ed. by Z. Yosida, Hokkaido University, Sapporo, Japan, August 1966, pp. 807-826
14. Hanagud, S., and B. Ross, "Propagation of Stress Waves in Snow," Paper presented at the 19th Alaskan Science Conference, Whitehorse, Yukon, Canada, August 1968
15. Hanagud, S., and B. Ross, "On Elastic Waves in a Locking Relaxing Solid," presented at the 6th International Congress on Acoustics, Tokyo, Japan, August 21-28, 1968 and published in Vol. IV, Section G, pp. G-1 through G-4 of the Conference Reports
16. Goodier, J. N., "On the Mechanics of Indentation and Cratering in Solid Targets of Strain-Hardening Metal by Impact of Hard and Soft Spheres; Technical Report 002-64, SRI Poulter Laboratories, Menlo Park, Calif., July 1964
17. Goodier, J. N., "On the Mechanics of Indentation and Cratering in Solid Targets of Strain-Hardening Metal by Impact of Hard and Soft Spheres," *Proc. 7th Symposium on Hypervelocity Impact*, Vol. III, February 1965, pp. 215-259
18. Hopkins, H. G., "Dynamic Expansion of Spherical Cavities in Metals," *Progress in Solid Mechanics*, Vol. 1, ed. by R. Hill and I. N. Sneddon, Pergamon Press, Oxford, England, 1960 pp. 84-164